Research Square

Preprints are preliminary reports that have not undergone peer review.
They should not be considered conclusive, used to inform clinical practice,
or referenced by the media as validated information.

Digitally Immune-Optimised Next-Generation Influenza Vaccine Provides Cross-Clade Protection Against Emerging H5Nx Viruses

Jonathan Heeney

jlh66@cam.ac.uk

University of Cambridge https://orcid.org/0000-0003-2702-1621

Joanne Marie Del Rosario

DIOSynVax Ltd.

Sneha Vishwanath

Laboratory of viral zoonotics, Department of Veterinary Medicine, University of Cambridge
https://orcid.org/0000-0001-9960-547X

Simon Frost

DIOSynVax Ltd., London School of Hygiene and Tropical Medicine, Microsoft Health Futures

Sneha Sujit

DIOSynVax Ltd.

Sruthika K Ashokan

DIOSynVax Ltd. https://orcid.org/0009-0008-6526-4839

Robert Vendramelli

Public Health Agency of Canada

Matteo Ferrari

DIOSynVax Ltd.

George Carnell

University of Cambridge https://orcid.org/0000-0001-8875-0989

Lucrezia Vianello

Istituto Zooprofilattico Sperimentale delle Venezie (IZSVe)

Matteo Pagliari

Istituto Zooprofilattico Sperimentale delle Venezie (IZSVe), University of Padua

Sami Ramzi

Istituto Zooprofilattico Sperimentale delle Venezie (IZSVe), University of Padua

Valentina Maria Panzarin

Istituto Zooprofilattico Sperimentale delle Venezie (IZSVe)

Andrea Fortin

Istituto Zooprofilattico Sperimentale delle Venezie (IZSVe)

Marta Vascellari
Istituto Zooprofilattico Sperimentale delle Venezie (IZSVe)
Thang Truong
Public Health Agency of Canada
Paul Tonks
University of Cambridge
Ana Liza Ortiz
University of Cambridge
Chloe Huang
University of Cambridge
Sebastian Einhauser
University of Regensburg
Michael Schachtner
University of Regensburg
Benedikt Asbach
University of Regensburg https://orcid.org/0000-0003-1056-8591
Nigel Temperton
University of Kent https://orcid.org/0000-0002-7978-3815
Ron Moss
DIOSynVax Ltd.
Matthew Davies
DIOSynVax Ltd.
David Moss
DIOSynVax Ltd.
Rebecca Kinsley
DIOSynVax Ltd.
Ralf Wagner
University of Regensburg
Darwyn Kobasa
Public Health Agency of Canada https://orcid.org/0000-0002-6371-7493
Francesco Bonfante
Istituto Zooprofilattico Sperimentale delle Venezie (IZSVe)

Article

Keywords:

Posted Date: May 16th, 2025

DOI: https://doi.org/10.21203/rs.3.rs-6647740/v1

License: This work is licensed under a Creative Commons Attribution 4.0 International License. Read Full License

Additional Declarations: Yes there is potential Competing Interest. J.M.D., S.B.S., S.K.A., G.W.C., M.F., M.D., D.M., R.K., R.M., R.W., and J.L.H. are employees or shareholders of DIOSynVax Ltd. S.F. is an employee of Microsoft. The sequences of the DVX antigens have been patented under UK Patent Application No. GB2414517.8, Influenza vaccines, PCT/GB2022/052534, and PCT/GB2024/052670 (Influenza Antigen Synergies patent).

Abstract

A panzootic of H5Nx avian influenza viruses has severely affected poultry and wild bird populations resulting in multiple mammalian spillovers, including human infections caused by antigenically distinct and diverse virus clades. The unpredictable nature of spillover events of antigenically drifted and/or reassorted H5Nx viruses hinders our ability to effectively respond retroactively to the heightened risk of human-to-human transmission. Stockpiled strain-specific H5 whole virus-based vaccines provide limited breadth and reduced efficacy. To address this problem, we computationally designed vaccine antigens that induce broad protective immunity. Mice immunised with the DVX-panH5Nx mRNA vaccine candidate generated robust immune responses across A/H5 clades and provided crucial cross-clade protection against lethal H5N1 challenge, including strains that have recently caused human infection. Furthermore, ferrets immunised with DVX-pan-H5Nx demonstrated superior protection and immune breadth when compared to an industry standard inactivated antigen derived from the WHO candidate virus vaccine A/Astrakhan/3212/2020 (H5N8), against a lethal heterologous challenge.

INTRODUCTION

A panzootic of high pathogenicity avian influenza viruses (HPAI) of the H5Nx subtype has affected poultry and wild birds in all continents except Oceania[1,2]. These viruses evolved from the H5N1 goose/Guangdong (Gs/Gd) lineage that emerged in China in 1997, spreading to over 108 countries, affecting more than 300 million birds and 70 different mammalian species worldwide[1,2]. Estimates suggest over 1000 H5Nx human infections with differing severity in morbidity and mortality have been caused by different clades of the A/H5 subtype globally[1–3]. Genetic and antigenically distinct clades have become endemic in certain regions. Sporadic infections of 2.3.4.4b H5Nx viruses have been detected in polar bears[4], farmed mink[5], foxes[6], goats[7], sea lions[8], domestic cats[9], and dogs[10] in recent years (**Fig.1**). Specifically, these clade 2.3.4.4b viruses continue to spread globally, displacing other clade viruses and reassorting with other Gs/Gd clades and local low pathogenic avian influenza (LPAI) viruses to produce a diverse range of genotypes[1,11,12]. In 2024, 2.3.4.4b H5N1 HPAI virus began spreading rapidly in dairy cattle in the United States and has since been identified in draining water reservoirs, the human food chain, and in dairy and poultry products, increasing the risk of human adaptation[2,13–16].

Combating unpredictability regarding which variant, clade, or reassortant will spill over to humans and establish successful human-to-human transmission, requires broader and more effective vaccines than the current industry standard of strain-specific-based products[13,17–19]. To address this problem, we utilised Digitally Immune Optimised Synthetic Vaccine (DIOSynVax) technology[20] to select cross-reactive antigens and combine different classes of the best antigens expressed as mRNA vaccine antigen payloads. The resulting mRNA vaccine candidate, DVX-pan-H5Nx, induced potent neutralising immune responses and cross-clade protection against diverse H5Nx viruses in animal models. Here we describe the antigen designs and their immunogenicity profile in a mouse model, and evaluated combined antigen payloads of hemagglutinin (HA), neuraminidase (NA), and matrix protein 2 (M2) in different animal

models. Subsequently, in pre-clinical models, we compared head to head, the breadth and protective efficacy of DVX-pan-H5Nx to the industry standard, adjuvanted whole inactivated virus (WIV) preparations based on a candidate vaccine virus (CVV) from clade 2.3.4.4b, A/Astrakhan/3212/2020 (H5N8). This study demonstrates the efficacy of a new paradigm in vaccine design by combining computational and structural vaccine antigen design technology to address the unpredictable, constantly evolving global pandemic threat of avian influenza.

RESULTS

In silico antigen design.

To develop a vaccine capable of eliciting a broader immune response to multiple clades of the A/H5 subtypes, we used the Digital Immune Optimised Synthetic Vaccine (DIOSynVax) technology previously described[20]. We targeted five influenza structural antigens representing hemagglutinin (HA), neuraminidase (NA), and matrix 2 (M2) of H5 subtype for digital designs, and immunologically down-selected five candidate vaccine antigens, two HA of the H5 subtype, henceforth referred as DVX-H5-1 and DVX-H5-2, NA of N1 and N6 subtype, henceforth referred as DVX-N1 and DVX-N6 respectively, and matrix M2 of type A Influenza viruses, henceforth referred as DVX-M2. NAs for N1 and N6 subtypes were selected as these were the most frequently observed subtypes in spillovers with fatal consequences in humans over the past decade (Fig. 1). For designing HA antigens representative of the H5 subtype, a dataset of non-redundant H5 sequences was compiled using the GISAID database[23–25] (Fig. 2a). DVX-H5-1 was designed utilising sequences from H5 clades that have caused human infection, while DVX-H5-2 was designed using only sequences from clade 2.3.4.4. For designing NA antigens representative of N1 and N6 subtypes, and an antigen representative of Influenza A M2, non-redundant datasets of N1 (Fig. 2c), N6 (Fig. 2e), and M2 (Fig. 2g) sequences respectively, were compiled using NCBI virus datasets[26]. Due to evolutionary associations between the input sequences and the evolution model used in our pipeline to generate these five antigens, these designs capture both the conserved as well as distinct epitopes of the input sequences to generate broad intra-subtype immune responses.

Immunogenicity of antigens as DNA immunogens in BALB/c mice.

Groups of BALB/c mice were immunised with one of the following DNA immunogens, DVX-H5-1, DVX-H5-2, DVX-N1, DVX-N6, and DVX-M2 to evaluate the breadth of immune responses (Fig. 2b, 2d, 2f, 2h). The immune responses induced by these antigens were compared with that generated in BALB/c mice immunised with DNA plasmids encoding sequences representative of wild-type strains (**Supplementary Table 2**). The wild-type strains for H5 were selected based on CVVs. N1 and M2 controls were selected based on strains used in the seasonal flu vaccine. The N6 control was selected such that it was the most phylogenetically distant to DVX-N6. Sets of naive mice were immunised with PBS as a negative control.

Mice immunised with DVX-H5-1 seroconverted and elicited higher neutralisation titres to pseudotype viruses (PV) from clade 2.1.3.2, and clade 2.2 in comparison to the rest of the groups. Moreover, DVX-

H5-1 mice had the highest number of responders to clades 1 and 2.3.2.1c compared to other groups (Fig. 2b). Mice immunised with DVX-H5-2 seroconverted to all clade 2.3.4.4 PV and showed titres that were not statistically different to mice immunised with HA antigens from wild-type strains (Fig. 2b). Moreover, the wild-type 2.3.4.4h clade HA control only elicited a homologous neutralisation response. HA antigens from wild-type strains representative of 2.3.4.4a and 2.3.4.4c were non-neutralising against PV representative of 2.3.4.4h. Neutralisation data demonstrated the breadth of DVX-H5-1 and DVX-H5-2 in comparison to HA antigens based on wild-type strains.

All mice immunised with DVX-N1 generated neuraminidase inhibition titres against all N1 PV of human, avian, and mammalian origin except for BNE/2018 (Fig. 2d). BNE/2018-immunised mice inhibited its homologous NA, but no inhibition was observed against any other tested PV. The DVX-N1 antigen elicited significant inhibition titres against N1 from different avian and mammalian virus strains (Fig. 2d). Similarly, most mice immunised with DVX-N6 inhibited all PV tested of human and avian origin (Fig. 2f). The NA antigen from ye/CHL/2013 (H7N6) inhibited only the homologous strain but no inhibition was observed against any other tested PV (Fig. 2f). These data support the wide breadth of our DVX NA antigens compared to selected wild-type N1 (Fig. 2d) and N6 (Fig. 2f) antigens.

Mice immunised with DVX-M2 generated appreciable binding titres (MFI > 10^2) against cells expressing (in gray boxes) the homologous antigen, and M2 proteins from BNE/2018 (H1N1) and KS/2017(H3N2) (Fig. 2h). No significant differences between DVX-M2 and the M2 of wild-type strains were observed.

Superior cross-clade neutralisation of computationally designed DVX-pan-H5Nx compared to combined whole inactivated wild-type virus-based antigens in mice.

With the advent of mRNA technology and its sweeping impact on the vaccine landscape[32–34], we produced our antigen constructs as an mRNA vaccine antigen payload, DVX-pan-H5Nx (Fig. 3a). Two strain-specific whole virus antigens based on WHO-recommended CVVs from clades 1 and 2.3.4.4b that have been approved for vaccine manufacture in the past were administered to evaluate their interclade neutralising activity compared to DVX-pan-H5Nx in mice (Fig. 3b, **Supplementary Table 5**). Post-immunisation sera from Day 63 (D63) from mice administered DVX-pan-H5Nx at D0 and D21 (Fig. 3b) revealed potent neutralisation responses across a H5 PV panel from different clades, including strains that caused bovine infections and outbreaks in Colorado[35], and the recent H5N1 clade 2.3.4.4b (genotype D.1.1) virus that caused a severe infection in an adolescent in British Columbia[36] (Fig. 3c). The H5 PV panel included representative viruses from different H5 Gs/Gd clades that are phylogenetically and antigenically distinct from each other (Fig. 1, **Supplementary Table 3**). Neutralising titres ≥ 10^3, (an arbitrary threshold of neutralisation potency in a pMN[20,27–30]), were observed in mice immunised with DVX pan-H5Nx against PV from the American non-goose Guangdong lineage (AM non-GS/GD), and from Gs/Gd clades 7.1, 1, 2.2, 2.2.1, 2.3.2.1a, 2.3.2.1c, 2.3.4.4a, 2.3.4.4b, 2.3.4.4c, and 2.3.4.4h (Fig. 3c). Mice immunised with A/Vietnam/1194/2004 (H5N1) (WIV_1) developed neutralisation titres > 10^3 only against clade 7.1 and 1 PV, while A/Astrakhan/3212/2020 (H5N8) ($WIV_{2.3.4.4b}$) developed titres against the

2.3.4.4a, 2.3.4.4b, and 2.3.4.4c, and not against 2.3.4.4h or any other clades tested. Neither WIV reached the titre, nor the cross-clade neutralisation exhibited by DVX-pan-H5Nx against all PV tested (Fig. 3c). The number of mice that responded above the defined IC_{50} titre threshold is depicted as heatmaps in Fig. 3d; demonstrating DVX-pan-H5Nx's superior immune breadth over whole inactivated CVV antigens.

We then determined inhibition of neuraminidase (N1 and N6) activity induced by DVX-pan-H5Nx. Neuraminidase inhibition in the range of $IC_{50} \sim 10^2 - 10^4$ was observed against N1 from seasonal strains such as VIC/2019, and VIC/2022, pandemic strains ENG/2009, and sw/ENG/2009, and from multiple species such as mink, avian, harbour seal, and the latest H5N1 case from British Columbia, a clade 2.3.4.4b D1.1 neuraminidase reassortant[37] (Fig. 3e, **Supplementary Table 4**). WIV_1 (with an N1 component) induced inhibition titres to less than half of N1 PV, with titres at least 100-fold lower than DVX-pan-H5Nx against all PV tested. This data supports the significantly superior responses induced by DVX-pan-H5Nx over standard WIV vaccines in terms of N1 inhibition. Additionally, DVX-pan-H5Nx elicited anti-N6 titres in the range of $IC_{50} > 10^3$ against avian N6, du/NgheAn/2019 (N6), and human SC/2014 (N6), and $IC_{50} \sim 10^2$ against ye/CHL/2013 (N6) (Fig. 3f, **Supplementary Table 4**). DVX-pan-H5Nx also induced binding antibodies against M2 protein from A/chicken/Hebei/326/2005 (H5N1) (Fig. 3g). The immunogenic role of M2 has been demonstrated by several independent studies[38–41].

Protective cross-clade efficacy of DVX-pan-H5Nx in lethal mouse H5N1 challenge models.

Following successful immunogenicity studies, vaccine efficacy in mice immunised with DVX-pan-H5Nx versus A/Astrakhan/3212/2020 (H5N8) ($WIV_{2.3.4.4b}$) was compared (Fig. 4a, **Supplementary Table 6**). $WIV_{2.3.4.4b}$ was specifically chosen as it is a strain for which a CVV vaccine has been pre-authorised for use in the event of an H5Nx outbreak in humans. Prior to challenge, mice were tested for serum neutralisation titres against each of the challenge viruses. Mice immunised with DVX-pan-H5Nx displayed titres ($IC_{50} \geq 10^3$) against A/British Columbia/PHL-2032/2024 (H5) (clade 2.3.4.4b), and A/Vietnam/1203/2004 (H5) (clade 1) (Fig. 4b). Titres were more modest for all groups against A/Cambodia/NPH230032/2023 (H5) (clade 2.3.2.1c). $WIV_{2.3.4.4b}$ only elicited titres against the clade 2.3.4.4b PV and was significantly inferior to DVX-pan-H5Nx against all PV tested, consistent with previous findings (Fig. 3c). Additionally, DVX-pan-H5Nx showed considerable N1 and N6 inhibition ($IC_{50} \geq 10^2$) against all PV tested, whereas the $WIV_{2.3.4.4b}$ mice did not inhibit any of the PV tested including the N8 PV despite having an N8 component (Fig. 4c).

We then proceeded to challenge mice with three H5N1 viruses from different clades (1, 2.3.2.1c, and 2.3.4.4b) that have recently caused human infections, thereby presenting the biggest pandemic threats (Fig. 1, **Supplementary Table 6**). Weight loss and clinical symptoms of influenza were observed during the 14-day study window or until mice were culled. There was 100% survival, supported by no weight loss or symptoms of influenza infection observed in mice immunised with DVX-pan-H5Nx against all viruses for the duration of the study demonstrating complete protection from multi-clade H5 HPAI challenge (Fig. 4d-f). In contrast, animals immunised with $WIV_{2.3.4.4b}$ only showed protection against the

matched 2.3.4.4b challenge (Fig. 4d); 67% survival with weight loss and clinical symptoms commencing 5 days post-challenge (dpc) against 2.3.2.1c H5N1 (Fig. 4e); and 50% survival with weight loss observed as early as 4dpc against clade 1 H5N1 (Fig. 4f). All mice from the naive group did not survive any of the challenges and were culled due to reaching humane endpoints as early as 5dpc (Fig. 4d-f).

The extent of protection conferred by DVX-pan-H5Nx compared to $WIV_{2.3.4.4b}$ immunisation was further characterised by determining infectious viral titres in lung and spleen. For this, 6 mice per group were culled 4dpc and tissues harvested. Virus titres in lung and spleen were below the limit of detection (LOD) in mice immunised with DVX-pan-H5Nx (Fig. 4d-f). In contrast, virus could be detected in the lungs of $WIV_{2.3.4.4b}$ mice challenged with clade 1 H5N1 (Fig. 4f). Significant virus titres were observed in lungs of naive mice (Fig. 4d-f) and the clade 2.3.4.4b virus was also detected in their spleens (Fig. 4d). These evidence suggest that DVX-pan-H5Nx protects mice against lethal challenge of divergent H5N1 viruses by limiting viral replication in the lungs, thereby minimising infection, which then correlates with survival.

DVX-pan-H5Nx elicits broad H5 neutralisation and NA inhibition in ferrets.

To correlate immunogenicity with efficacy in a well-characterised and widely accepted model of human influenza infection[42,43], we administered DVX-pan-H5Nx to ferrets and compared it to adjuvanted inactivated antigen A/Astrakhan/3212/2020 (H5N8) ($WIV_{2.3.4.4b}$). All ferrets were immunised using the same schedule used to evaluate immunogenicity in mice (Fig. 5a, **Supplementary Table 8**). Serum collected from DVX-pan-H5Nx ferrets on D42 showed appreciable neutralising titres against H5 PV similar to that observed in mice (Fig. 5b). Interestingly, there was a significant difference in neutralisation of clades 2.2 and 2.2.1 between DVX-pan-H5Nx and $WIV_{2.3.4.4b}$, where the WIV showed no reactivity. As expected, both DVX-pan-H5Nx and $WIV_{2.3.4.4b}$ induced considerable serum neutralisation ($\sim 10^4$) against all 2.3.4.4 PV tested, with a higher response of the WIV group against 2.3.4.4a/b PV, while the DVX-pan-H5Nx ferrets showed higher titres against 2.3.2.1c PV (Fig. 5b). We assayed for anti-N1 and anti-N6 activity of DVX-pan-H5Nx, and neuraminidase inhibition titres ($IC_{50} > 10^2$) were observed against majority of N1 and N6 PV tested (Fig. 5c). Hemagglutination inhibition (HI) revealed comparable seroprotective HI titres in DVX-pan-H5Nx and $WIV_{2.3.4.4b}$ groups against 2.3.4.4 viruses (Fig. 5d-e, **Supplementary Table 9**). Notably, for DVX-pan-H5Nx sera, we recorded 4-8-fold higher HI titres to viruses from clades 1 and 2.2.1, while for 2.3.2.1c and 2.3.4.4c, a 2-fold increase was evident in $WIV_{2.3.4.4b}$, again emphasising the breadth of cross-reactivity induced by DVX-pan-H5Nx compared to the narrow specificity of $WIV_{2.3.4.4b}$ (Fig. 5d). After peak responses on day 42, $WIV_{2.3.4.4b}$ and DVX-pan-H5Nx groups showed decreased HI titres against the challenge strain of 1:40 and 1:15, respectively on day 50 (Fig. 5e), suggesting that correlates of protection other than HI titres affect efficacy. Both groups seroconverted as measured by ELISA assays (Fig. 5f, **Supplementary Figs. 1–2**), with sera from the $WIV_{2.3.4.4b}$ group showing superior antibody binding. Nonetheless, despite lower levels of antibodies detected to clade 1 and clade 2.3.2.1c antigens by the DVX-pan-H5Nx group (Fig. 5f), the same sera recorded higher median values in both pMN and HI assays, suggesting greater specificity for the neutralising epitopes of hemagglutinin. To evaluate the induction of T-cell responses that were cross-reactive to the challenge

virus, ferret PBMCs were stimulated with whole inactivated A/chicken/Italy/23VIR3799-1/2023 (H5N1). Representative IFN-γ ELISpot results for both vaccine groups (Fig. 5g, left panel, **Supplementary Fig. 3**) showed more spot-forming units (SFU) when compared to naive controls (Fig. 5g, right panel). Taken together, these findings demonstrated that DVX-pan-H5Nx elicited robust B-cell responses including broad neutralisation across diverse H5 clades, N1 and N6 inhibition, as well as T-cell responses.

DVX-pan-H5Nx elicits superior efficacy compared to WIV $_{2.3.4.4b}$ against HPAI 2.3.4.4b challenge in ferrets.

Vaccine efficacy in ferrets was then assessed by heterologous challenge with A/chicken/Italy/23VIR3799-1/2023 (H5N1), a representative virus of the current panzootic of 2.3.4.4b, also containing a 4-amino acid difference in the HA with $WIV_{2.3.4.4b}$ (**Supplementary Fig. 4**). During the 14-day post-challenge (dpc) monitoring period, all naive control ferrets, and 50% of animals immunised with $WIV_{2.3.4.4b}$, reached clinical endpoint or succumbed to disease by 8dps. In contrast, only 1 animal from the DVX-pan-H5Nx group reached the humane endpoint requiring culling (Fig. 6a). Interestingly, the risk of death (calculated by the Cox proportional hazard model) was estimated to be 3.41 times higher (hazard ratio (HR):0.182) in animals receiving $WIV_{2.3.4.4b}$, representing a surrogate of a commercially available vaccine stockpile, compared to the digitally designed DVX-pan-H5Nx (HR):0.05. Moreover, less weight loss (Fig. 6b) and higher temperatures (Fig. 6c) on days indicated were observed in DVX-pan-H5Nx compared to $WIV_{2.3.4.4b}$ animals. In particular, DVX-pan-H5Nx mRNA immunisation better protected ferrets from weight loss in comparison $WIV_{2.3.4.4b}$, as indicated by the significantly higher weight of animals between 4-8dpc (Fig. 6b). Evidence of clinical disease was first detected at 3dpc in naive controls, and at 1dpc in some of the vaccinated animals, with peak severity recorded 8-9dpc (all groups Fig. 6d). In comparison to naive ferrets, DVX-pan-H5Nx achieved significantly lower clinical scores between 5-8dpc while significantly lower scores were observed only for 5-6dpc in the $WIV_{2.3.4.4b}$ ferrets. Superior clinical protection in DVX-pan-H5Nx animals combined with temperatures that were significantly higher than those of WIV-immunised ferrets on 4, 6, and 7dpc was observed (Fig. 6a-e). Notably, DVX-pan-H5Nx ferrets demonstrated the lowest cumulative clinical scores, followed by the 50% of animals in the $WIV_{2.3.4.4b}$ group that survived (Fig. 6e, **Supplementary Fig. 5**). All survivors had improved clinical outcomes reflected by less weight loss and lower clinical scores (Fig. 6a-e). Interestingly, despite superior clinical protection, higher shedding was observed in some DVX-pan-H5Nx ferrets in the early days of infection (prior to 6dpc) compared to $WIV_{2.3.4.4b}$ (Fig. 6f). This decreased from 6dpc onwards while in naive disease progressors, viral RNA copies remained high (Fig. 6f), suggesting that immunisation-related survival was linked to low viral RNA loads during the latter part of the challenge window. In ferrets that survived, there were no significant differences in viral RNA loads in immunised animals. Viral assays from post-mortem samples from bronchoalveolar lavages, lung, liver, spleen, and pancreas, demonstrated low values (below the limit of detection) in all survivors (14dpc) (Fig. 6g). For non-survivors, titres are shown from post-mortem samples taken at the time of death. Additionally, greater T-cell responses in DVX-pan-H5Nx vaccinated animals was observed post-challenge (Fig. 6h, **Supplementary Fig. 6**), suggesting more robust effector immune responses that facilitated viral

clearance. Histopathology revealed a spectrum of lesions depending on the day of euthanasia post-infection. The time of sacrifice was determined by the clinical score severity. Animals with early progressive clinical disease tended to have a higher degree of brain inflammatory infiltrates and/or more severe lung inflammation while less severe interstitial changes were present in the animals that survived (**Supplementary Table 11**).

DISCUSSION

The global spread and evolutionary plasticity of H5Nx influenza has enabled it to spread and cause disease in hundreds of wild bird and poultry species, as well as over 70 mammalian species including humans. Estimates have suggested that over 1,000 human infections have occurred with significantly higher morbidity and mortality observed especially from clade 2.3.2.1c/e in Southeast Asia, the cause of human infections with the highest human fatality rates[44] in 2024/2025. With the spread of H5 2.3.4.4b in dairy cattle and poultry in the United States, viral RNA has been documented in water reservoirs and the human food chain[15,16,45]. The ongoing genetic diversity with viral reassortment through inter-species transmissions underscores the urgent need for innovative vaccine solutions. Significant variables make it extremely difficult to predict which H5 variant may acquire optimal adaptations for efficient human-to-human transmission, thereby hampering the process of wild-type virus isolate selection for vaccine development using currently licensed influenza vaccine manufacturing methods. This, combined with the economic cost of pre-purchasing millions of doses of a pre-authorised H5 vaccine from licensed manufacturers to stockpile, is an additional financial risk and barrier, especially if current commercially available vaccines have limited protection against new H5 variants that adapt to spread rapidly between humans.

To address this problem, we took a different approach to the current wild-type virus strain selection. Using the global sequence database of H5Nx viruses in animals and humans over the last 20 years, we computationally engineered HA, NA, and M2 antigens and evaluated these antigens for the induction of broad anti-H5Nx immune responses in mice and ferrets. Subsequently in both mouse and ferret influenza challenge models, we compared the vaccine protection afforded by a clade 2.3.4.4b strain based whole inactivated WHO candidate virus vaccine representing a current pre-pandemic stockpile candidate, to our digitally immune optimised DVX-pan-H5Nx mRNA vaccine candidate.

Complete protection of mice immunised with DVX-pan-H5Nx in challenge models covering three different clade H5N1 viruses with the highest pandemic potential was demonstrated (**Fig. 4**). Mice that survived all challenges had no detectable virus in their lungs and spleen indicating viral clearance and/or non-replication of virus during the height of infection. Likewise, immunised and naive ferrets were challenged with a heterologous clade 2.3.4.4b H5N1 and monitored for immune responses and vaccine efficacy. In both animal models, results revealed superior clinical protection afforded by DVX-pan-H5Nx in comparison to an inactivated whole virus antigen based on the WHO CVV A/Astrakhan/3212/2020 (H5N8) ($WIV_{2.3.4.4b}$). $WIV_{2.3.4.4b}$ only afforded narrow clade-specific protection, with decreased efficacy observed against clade 2.3.2.1c (challenge virus used was a 2:6 reverse genetic virus HA and NA from

A/Cambodia/2023 and internal genes from A/Astrakhan/3212/2020) and clade 1 viruses. Moreover, neuraminidase inhibition exhibited by DVX-pan-H5Nx (**Fig. 4c**) may have played an important role in improving survival outcomes of DVX-pan-H5Nx immunised animals. In addition to superior immune breadth *in vitro*, ferrets vaccinated with DVX-pan-H5Nx developed more potent humoral responses to the challenge virus, a highly desirable quality for a vaccine in the context of a pandemic outbreak. While HI titres of 1:40 to a specific challenge virus are recognised as an important correlate of influenza vaccine efficacy, these findings indicate that heterologous vaccine protection can be achieved with DIOSynVax technology in the presence of lower HI titres. Interestingly the response to infection was more robust in the DVX-pan-H5Nx group in the febrile phase (**Fig. 6c**), with less severe clinical symptoms (**Fig. 6d-e**).

The economics and global human health benefits of having broadly protective pre-pandemic vaccines stockpiled and ready for deployment early in a human pandemic far outweigh deployment of a mismatched vaccine with lower efficacy that may facilitate vaccine escape. Pre-pandemic access to broadly protective vaccines pre-empts the delays of post-outbreak “reactive” responses to triggering manufacturing vaccines based on the emerging wild-type strain after the outbreak and spread of a highly transmissible virus has begun[46–49]. In addition, the pre-pandemic availability of broadly protective vaccines increases the opportunity for containment and eradication, avoiding the costly cycle of annual (or semi-annual) vaccine reformulation and production in response to evolving viral threats in a post-pandemic to endemic scenario. Even with the continuous evolution of A/H5 worldwide, there has been no need to update the composition of DVX-pan-H5Nx to date, giving it a considerable advantage as a global H5Nx stockpiled vaccine solution to the threat posed by avian influenza. Given the findings reported here, further clinical development of this DVX-panH5Nx vaccine candidate is warranted for pre-pandemic preparedness to protect from the diverse clades and potential reassortant viruses that may adapt to cause human to human transmission from the extraordinary and ongoing evolution of A/H5 influenza.

METHODS

In-silico design of vaccine antigens

The nucleotide sequences of hemagglutinin (HA), neuraminidase (NA), and Matrix protein (M2) of H5Nx subtype were obtained from the GISAID[23–25] database. The sequence datasets were utilised to generate unique antigen sequences for HA, NA, and M2 which are phylogenetically closest to all the input sequences in comparison to any sequence in the downloaded dataset. The DVX-H5-1, DVX-N1, DVX-N6, and DVX-M2 designs were generated using sequences submitted up to April 2019 and DVX-H5-2 was generated using sequences submitted up to December 2020. In brief, for HA, NA, and M2, the sequences were trimmed to the coding regions and filtered for redundancy at 95% sequence identity. Using the MAFFT[50] algorithm, multiple sequence alignment (MSA) of HA, NA, and M2 was generated with default parameters. Phylogenetic trees for HA, NA, and M2 were produced using the previously generated MSA using IQ-tree algorithm[51]. The optimal nucleotide model for phylogenetic tree generation was chosen

according to Bayesian information criteria (BIC) score. The phylogenetic tree and MSA were used as input to Hyphy[52] to generate antigens.

Production of plasmids for in vivo DNA immunogenicity studies and pseudotype assays

For selection of immune-optimised antigens *in vivo*, DVX-H5-1, DVX-H5-2, DVX-N1, DVX-N6, DVX-M2, and wild-type hemagglutinin (H5), neuraminidase (N1, N6), and M2 antigens as controls (**Supplementary Table 2**) were cloned in pEVAC plasmids (GeneArt). Additionally, wild type H5, N1, and N6 were also cloned in pEVAC or pI.18 plasmids to produce DNA for transfections to make pseudotyped viruses (**Supplementary Tables 3-4**) for pMN and pELLA. Plasmids were transformed via heat-shock into competent DH5-α *E. coli* (Invitrogen, EC0112) cells. DNA was extracted from bacterial cultures using the Qiagen plasmid DNA extraction kit (QIAprep® Spin Miniprep Kit, 27106) for pseudotype production and via the EndoFree® Plasmid Mega Kit (QIAGEN, 12381) for production of DNA for immunogenicity studies. Plasmid DNA was then quantified using UV spectrophotometry (Nanodrop™ 1000, ThermoFisher, UK) and a sequence integrity check was done by Sanger sequencing (Source Bioscience, UK).

Production of mRNA vaccines for in vivo immunogenicity and efficacy studies in mice and ferrets

The DVX antigens were made into mRNA in Lipid Nano Particles (LNP) by etherna (Niel, Belgium). Briefly, the mRNA vaccine candidates were transcribed *in vitro* from a linearised plasmid DNA template encoding 5’ and 3’ untranslated regions and a polyadenosine tail. Co-transcriptional capping was performed using CleanCap AG (Trilink). The LNP was formulated using the S-Ac7-DOG ionisable lipid and prepared as described previously[53].

Production of lentiviral pseudotyped viruses

Human Embryonic Kidney cell line (HEK293T/17) (ATCC-CRL-11268™) was obtained from American Type Culture Collection (ATCC). Cells were propagated and maintained in complete Dulbecco’s Modified Essential medium (1X DMEM-GlutaMax (Gibco™, 31966-021) supplemented with 10% (v/v) Fetal Bovine Serum (FBS) (Thermo Scientific, A5256801, heat inactivated at 56°C) and 1% (v/v) Penicillin/Streptomycin (Thermo Scientific, 15140-122)). Pseudotype virus was produced as described previously[27,31] using HEK293T/17 cells seeded in 6-well tissue culture plates (Griener Bio-one, 657160) in complete DMEM. The cells were transfected with pEVAC or pI.18 plasmids encoding HA or NA. These plasmids were co-transfected with p8.91, Luciferase reporter plasmid (pCSFLW), and FuGENE® HD (Promega, E231A). For transfection of NA plasmids, an additional H11 gene encoding plasmid (A/red shoveler/Chile/C14653/2016) was used. For HA plasmids, 1 unit per well of exogenous neuraminidase (Merck, N2876) was added 14-16 hours post transfection. After 72 hours of incubation at 37ºC, 5% CO_2, pseudotype viruses were harvested by collecting the supernatant. Supernatant was filtered using a 0.45 µm Millex® MCE syringe filter (Merck Millipore, SLHAR33SB) and stored at –80°C.

Viruses

For the mouse challenge study, the following three HPAI H5N1 viruses were selected: i) A/British Columbia/PHL-2032/2024 (clade 2.3.4.4b; GISAID EPI_ISL_19548836), ii) A/Cambodia/NPH230032/2023 (clade 2.3.2.1.c; GISAID EPI_ISL_17024123), and iii) A/Vietnam/1203/2004 (clade 1; ABP51977.1). A/British Columbia/PHL-2032/2024 was isolated by passage of a tracheal aspirate sample on MDCK cells and passaged twice on MDCK to generate a P3 stock. A/Cambodia/NPH230032/2023 (KHM/2023 HN), a recombinant virus containing the HA and NA of A/Cambodia/NPH230032/2023 in a background of other genes derived from A/Astrakhan/3212/2020, was generated by reverse genetics, using the previously described protocol[54] and was passaged on MDCK cells. A/Vietnam/1203/2004, was kindly provided by Yoshihiro Kawaoka, University of Wisconsin-Madison, and passaged on MDCK cells. All viruses were titred by standard plaque assay on MDCK cells using MEM/1% Seaplaque agar (Lonza) overlay containing 0.75 µg/ml TPCK-trypsin (Sigma) and 0.1% BSA (Gibco).

The HPAI H5N1 A/chicken/Italy/23VIR3799-1/2023 (EPI_ISL_19767156) virus belonging to the 2.3.4.4b clade was selected for the ferret challenge. The following A(H5) HPAI viruses were used as HAI antigens to test the breadth of reactivity of sera collected from vaccinated ferrets: i) H5N1 A/Vietnam/1194/2004 (clade 1; EPI_ISL_30632), ii) H5N1 A/turkey/Turkey/2005 (clade 2.2.1), iii) IBCDC-RG6 A/Anhui/1/2005 (2.3.4 clade; EPI_ISL_24603), iv) IDCDC-RG43A A/gyrfalcon/Washington/41088-6/2014 (2.3.4.4c clade; EPI_ISL_173878), v) IDCDC-RG71A A/Astrakhan/3212/2020 (2.3.4.4b clade; EPI_ISL_13655139), vi) IDCDC-RG63A A/duck/Bangladesh/17D1012/2018 (2.3.2.1a clade; EPI_ISL_331119), and vii) A/duck/Vietnam/NCVD-1584/2012 (H5N1) (NIBRG-301) (NIBSC-17/142). The challenge virus was isolated by inoculation of specific-pathogen free (SPF) (Charles Rivers Laboratories) 9-to-11 day-old embryonated chicken eggs. Eggs were incubated for 72 hours at 37°C and candled daily. Dead embryos were chilled overnight at 4°C and allantoic fluids were harvested and tested by the hemagglutination (HA) test. Positive fluids were tested for the presence of bacterial contamination and stored at –80 °C.

Virus infectivity titration

Madin-Darby Canine Kidney (MDCK) cells (ATCC, CCL-34) were cultured at 37°C in a 5% CO_2 incubator in DMEM (Gibco, 41695-039) supplemented with 10% fetal calf serum (FCS) (Sial, yourSIAL-FBS-SA), 1% of a 2:3 (v/v) penicillin-streptomycin solution (10,000 Unit/mL) (Euroclone-ECB3001D) and a 1:3 (v/v) nystatin solution (Sigma-Aldrich, N1638) (10,000 Unit/ml) in Dulbecco's phosphate-buffered saline (DPBS) (Sigma- Aldrich, D8537).

Virus titrations were performed on confluent monolayers of MDCK cells, seeded at $3.75x10^4$ cells per well in 96-well plates (Corning, 3596). Briefly, after 24-hours incubation, confluent cell monolayers were washed and incubated for 1 hour at 37°C in a 5% CO_2 incubator with 50 µL of serial dilutions of the virus stock in cell culture medium deprived of FCS. After the incubation, 100 µL of the same medium was added to the inoculum in each well. After 72 hours, the medium was removed and cells were fixed in 4% paraformaldehyde (PFA), for 30 minutes at 4°C. Upon removal, cells were permeabilised by incubation with a 0.5% Triton X-100 (Sigma/Merck, T8787) PBS solution for 10 minutes. Immunostaining of infected

cells was performed by incubation of a mouse anti-Influenza A monoclonal antibody mix (1:4000) (Merck Millipore, MAB8257 and MAB8258 1:1) for 1 hour, followed by a 1-hour incubation with peroxidase-labeled goat anti-mouse antibodies (1:1000) (Jackson ImmunoResearch, 115-035-003) and a 7 min incubation with the TrueBlue™ (SeraCare, 5510-0030) peroxidase substrate. Solution of 1% bovine serum albumin (BSA) (Sigma/Merck, A9647) and 0.05% Tween-20 (Sigma/Merck, P2287) in PBS was used for the preparation of working dilutions of immuno-reagents. After the removal of the monoclonal antibody mix, wells were washed 4 times with the 0.05% Tween-20 PBS solution. For the titration of virus in organ supernatants, the protocol adopted to titrate the viral stock was modified to reduce cell toxicity through removal of the inoculum after incubation and washing with PBS before the addition of 150 µL of culture medium. The median tissue culture infectious dose ($TCID_{50}$) was calculated based on the Reed-Muench method[55].

In vitro expression of candidate vaccine antigens

The DNA and mRNA vaccine antigens were checked for *in vitro* expression via Flow cytometry. Briefly, HEK293T/17 cells were seeded in either 6-well ($2.1x10^5$ cells/well) for DNA or 96-well plates (3×10^6 cells/well) for mRNA expression. Next day, the cells were transfected with DNA using FugeneHD and mRNA using Lipofectamine MessengerMAX™ (Invitrogen™ LMRNA003). Untransfected “cells only” control was also included. The plates were incubated for 24 hours (mRNA) or 48 hours (DNA) at 37°C, 5% CO_2. Cells were harvested and washed twice with FACS buffer (1% FBS in PBS). Immune sera or monoclonal primary antibodies (mAbs) were added to the cells and incubated for 30 minutes at room temperature. After incubation, cells were washed again and an Alexa-Fluor 647 labelled anti-mouse (Invitrogen, A32728) or anti-human (Invitrogen, A21445) IgG secondary antibody was added to the plate followed by incubation for 30 minutes in the dark. Plates were washed and read using AttuneNxt Flow cytometer (Invitrogen, UK). “Cell only” data was subtracted from all wells and values were plotted as Median Fluorescence Intensity (MFI) values.

Animal immunogenicity and efficacy studies

Ethics

Mouse immunogenicity studies were approved by the Animal Welfare Ethical Review Body (AWERB), University of Cambridge (Project license PP9157246). Studies were conducted per UK Home Office regulations under the Animals (Scientific Procedures) Act 1986 (ASPA) and results are reported according to the ARRIVE Guidelines[56].

Mouse challenge studies were conducted as outlined in the Animal Use Document Application H-23-004, “Evaluation of vaccine candidates against HPAI H5N1 influenza”. This was approved by the Canadian Science Centre for Human & Animal Health - Animal Care Committee (CSCHAH - ACC) in accordance with the Canadian Council on Animal Care (CCAC).

Animal experimental procedures in ferrets were conducted in strict accordance with the Decree of the Italian Ministry of Health n. 26 of 4 March 2014 on the protection of animals used for scientific purposes, implementing Directive 2010/63/EU, and approved by the Institute's Ethic Committee (protocol n. 4/19 obtained on the 15/1/2020). Animal experiments were approved by the Ministry of Health (709/2020-PR, further amended by 5351-24/02/2025-DGSAF-MDS-P).

Mouse Immunogenicity studies

*For all mouse immunogenicity studies, 6-8 week-old female BALB/c mice were obtained from Charles River Laboratories and housed in separate groups of 6 mice each at the University Biomedical Services, University of Cambridge. For DNA immunogenicity studies, six mice (one group per antigen) were immunised subcutaneously (SC) on the rear flank with 50 µg DNA encoding DVX antigens and controls (**Supplementary Table 2**). For mRNA immunogenicity studies, DVX-pan-H5Nx and controls were injected intramuscularly in mice (6 mice per vaccine antigen) (**Supplementary Table 5**). The mice were culled at specified timepoints and terminal blood samples were collected. Serum was processed by heat-inactivation at 56°C to deactivate complement, and stored at -20°C for serology.*

Mouse Challenge studies

Six week old BALB/c mice (Charles River, Canada), equally divided between males and females, were allocated at Biosafety level 2 (BSL2) in the animal facility of the National Microbiology Laboratory in Winnipeg (NML), MB (Public Health Agency of Canada). At 7 weeks of age, 108 mice (54 males and 54 females) were divided in sets of three (one for each challenge virus) with each set consisting of 36 mice (18 males and 18 females). Each set was vaccinated with three different vaccine formulations (12 mice; 6 males and 6 females per vaccination group) (**Supplementary Table 6**), on days 0 and 21, and immunised by two intramuscular injections of vaccine, each given in 50 µl PBS to the quadriceps muscle of each hindlimb. Prior to virus challenge, mice were transferred to the BSL4 containment laboratory (NML) and housed in groups of 3 animals per HEPA-filtered cage. On day 49, each set was challenged with three HPAI H5N1 viruses (**Supplementary Table 6)** Mice were anesthetised using isoflurane delivered in 5% O_2 and $10LD_{50}$ (50% lethal dose) of virus in 50 µL neat MEM delivered by intranasal instillation. Four days post-challenge, 6 mice from each set (3 males and 3 females) were sacrificed to determine the influenza viral load in the lungs and spleens. The remaining 6 mice (3 males and 3 females) from each set were monitored for weight and clinical evaluations for 14 days or until an animal reached the mandated clinical endpoint. On day 63 (14dpc), all surviving mice were culled.

Viral titres in tissues were determined by $TCID_{50}$ assay. Frozen samples (-80°C) were thawed, weighed, placed in neat MEM, and homogenised with a 5 mm stainless steel bead in a Bead Ruptor Elite Tissue Homogenizer (Omni) for 30 seconds at 4 m/s. Homogenates were clarified by centrifugation at 1500*xg* for 10 minutes and ten-fold serial dilutions in MEM/0.1% BSA were added in triplicate to washed confluent MDCK cells in 96-well plates with MEM containing 0.1% BSA and 0.5 µg/mL TPCK-trypsin.

Cytopathic effect was read three days post-infection and $TCID_{50}$ gram of tissue were calculated by the method of Reed and Muench[55].

Clinical evaluation of mice during challenge window once daily. Clinical signs including weight loss, respiratory distress, ruffled fur, and hunched posture were scored. The humane endpoint was based on cumulative clinical score or weight loss above 25% of initial body weight or any signs of CNS infection including ataxia, paralysis, or loss of righting reflex.

Ferret Challenge study

Type A Influenza antibody-free male ferrets (*Mustela putorius furo*), 16 weeks of age, were purchased from a commercial supplier in Europe, allocated in the Biosafety Level 2 (BSL2) animal facilities of the Istituto Zooprofilattico Sperimentale delle Venezie (IZSVe), Legnaro, Italy, and identified with subcutaneous implantation of the Mini Thermochip sensors (MSD Animal Health, UIN 386923). Animals were quarantined for 2 weeks and enrolled for the study upon testing negative for the presence of type A influenza antibodies. At 19 weeks of age, 18 ferrets were vaccinated with three different formulations (**Supplementary Table 8**). Vaccination dose for $WIV_{2.3.4.4b}$ was adapted from literature[57–59]. All ferrets were vaccinated twice, on day 0 and on day 21 (**Fig. 5a**), receiving a total of 0.8 mL of formulation via three intramuscular (IM) injections at distinct sites at the level of the hind legs. Blood samples were collected from each ferret on days 0, 21, 42, 50, and 64. On day 47, the animals were transferred into Biosafety Level 3 (BSL3) animal facilities to allow for acclimatisation before the challenge. Each HEPA-filtered isolator (Montair, HM 1900) housed 2 animals. On day 50, ferrets were challenged through inoculation via the intranasal (IN) route with 200 µL of allantoic fluid containing 10^5 $TCID_{50}$ of the challenge virus. The challenge required that ferrets were maintained under surgical anaesthesia induced by an intramuscular injection of a solution comprising Nimatek® (100 mg/mL ketamine hydrochloride) and Domitor® (1 mg/mL medetomidine hydrochloride) at a ratio of 1:1 (v/v), with an injection volume equal to 80 µL/kg of body mass. Anesthesia was reverted by an intramuscular injection of Antisedan® (5 mg/ml atipamezole hydrochloride) to antagonise the action of the α-2 agonist Domitor®.

Nasal washes were collected under surgical anesthesia from each group of ferrets on days 2, 3, 4, 6, 8, 10 and 12 post-challenge and were immediately stored at -80°C. Briefly, 1 mL of PBS was inoculated in each nostril and about 1.5 mL of nasal wash was collected in total for each animal in a 50 mL conical tube. Necropsy was conducted on both deceased and sacrificed ferrets at the end of the study. Ferrets were examined at the macroscopic level for the presence of lesions and a bronchoalveolar lavage (BAL) was carried out. Briefly, a catheter was placed in the trachea and 10 mL of PBS was injected in the lungs and about 5 mL of fluid was recovered and stored at – 80°C. Moreover, the following organs were collected: cranial lung lobe, medial lung lobe, spleen, liver, brain, and pancreas. All organs were sampled and fixed in 10% neutral buffered formalin to perform histopathological and immunohistochemical analyses. Specimens from all organs, and a part from the brain, were stored at -80°C for virological

analyses. On day 64, two weeks after the challenge, all surviving ferrets were sacrificed under surgical anaesthesia by terminal exsanguination via cardiac puncture.

Clinical evaluation of ferrets during the challenge window

Temperature, body weight, and presence of clinical signs were monitored daily beginning three days before the challenge and for 14 days after the challenge. The temperature was recorded daily with the SureSense™ scanner (MSD Animal Health, HRPG1N) before the collection of samples. Clinical evaluation was carried out daily, at the same hour and was standardised through the adoption of a scoring system grading signs of disease as follows: 0 – alert and reactive subject irrespective of external stimulation; absence of respiratory signs; 1 – mild depression of the sensorium, reduced exploratory activity, engagement with the other ferret mate and reduction in the activity levels in response to external stimulation; nasal discharge or occasional sneezing; 2 – moderate depression of the sensorium, lethargy, exploratory activity and engagement with the other ferret mate are strongly reduced and are triggered only in response to external stimulation; frequent sneezing and/or laboured breathing; 3 – alterations of the sensorium, state of stupor, hyperexcitability, marked depression, tremors and/or reduced tone of the hind legs, abnormal interaction in response to external stimulation (e.g. stereotypic movements, aggressivity in tame subjects), and dispnoea; 4 – severe depression, severe neurological signs (e.g. ataxia, torticollis), inability to walk or feed; severe dispnoea and diaphragmatic breathing. The humane endpoint (HEP) was reached when animals were either assigned a score of 4, or in case of weight loss ≥ 20% of initial body weight (day 0).

Extraction of viral RNA and virus quantification by digital droplet RT-PCR

Nasal washes and BAL were centrifuged for 2 min at 2000*xg*. Tissue samples were weighed and homogenised on a TissueLyser II (Qiagen) in a 1:10 (w/v) ratio with PBS supplemented with 1% of a 2:3 penicillin-streptomycin solution (10,000 Unit/mL) (Euroclone-ECB3001D) and a 1:3 nystatin solution (Sigma-Aldrich, N1638) (10,000 Unit/mL). Homogenates were centrifuged at 10000*xg* for 1 min. Automated nucleic acid purification from all samples was performed using the MagMax CORE Nucleic Acid Purification Kit (Applied Biosystems) on a KingFisher Flex (ThermoFisher Scientific) according to manufacturer recommendations (workflow 'Simple'). Samples were subjected to viral genome quantification by digital RT-PCR (dRT-PCR) employing an oligonucleotide set targeting type A Influenza Viruses as previously described[60]. The PCR reaction mix consisting of the QIAcuity OneStep Advanced Probe Kit (Qiagen, 250131), 0.6 nM primers, 0.4 nM probe and 4 µL template was assembled with a Myra Liquid Handling System (Bio Molecular Systems, MYRA-LHS50) on 8.5k nanoplates. Amplification on a QIAcuity Digital PCR System (Qiagen, 911035) consisted of a reverse transcription step at 50°C for 40 min, reverse transcriptase (RT) inactivation at 95°C for 2 min, and 45 cycles of denaturation at 95°C for 5 sec and annealing/extension at 62°C for 1 min. Data were analysed with the QIAcuity Software Suite v. 2.5.0.1, with automatic threshold setting. Quantification data were converted to genome copies per 1 mL nasal/bronchoalveolar wash (GC/mL).

Histopathology

Following fixation, tissues underwent standard paraffin embedding and processing before hematoxylin and eosin (H&E) staining. Tissue pathology, e.g., for lungs - lesions, interstitial pneumonia, mononuclear phagocytosis, intrabronchial and intrabronchiolar inflammation, bronchial and bronchiolar epithelial cell necrosis, perivascular oedema, alveolar oedema, and neutrophil margination; and for brain – lymphocytic infiltration in the neuroparenchyma, encephalitis, gliosis, neuronophagia, and necrosis, was scored in blinded fashion in grades of 0 (absent), 1 (mild), 2 (moderate), to 3 (marked).

Serological investigations

Pseudotype neutralisation assay (pMN)

Serum neutralising titres post-immunisation against a H5 pseudotype virus panel (**Supplementary Table 3**) were determined via pMN as described previously[27]. Briefly, in a Nunc™ 96-well plate (Thermo Scientific™, 136101), starting at a 1:100 dilution, serum samples were serially diluted two-fold or three-fold in complete DMEM across the plate. Control wells consisting of “pseudovirus only” (equivalent to no neutralisation) and “cells only” (equivalent to 100% neutralisation) were included. H5 pseudotype virus ($1.0x10^6$ RLU (Relative luminescence unit)) was added to all wells except cells only wells and plates were incubated for 1 hour at 37°C, 5% CO_2. After incubation, $1.5x10^4$ HEK293T/17 cells were added to all wells and plates were incubated for 48 hours at 37°C, 5% CO_2. Supernatant was discarded and 1:1 diluted Bright-Glo™ luciferase assay substrate (Promega, E2620) in PBS (Thermo Scientific,10010023) was added per well for 5 minutes. The plates were read using GloMax® Navigator (Promega) using the Promega GloMax® Luminescence Quick-Read protocol and values were calculated as relative luminescence units/mL (RLU/mL).

Pseudotype Enzyme Linked Lectin Assay (pELLA)

Neuraminidase inhibition titres against an N1, and N6 pseudotype virus panel (**Supplementary Table 4**) were determined via pELLA as described previously[31]. Briefly, Nunc™ clear Maxisorp plates (Thermo Scientific™, 439454) were coated with 25 µg/mL Fetuin (Sigma, F3385) and incubated at 4°C. Next day, 1:100 dilution of serum samples were serially diluted two-fold in sample diluent (SD) (1% (w/v) Bovine Serum Albumin (BSA) (Merck, A2153) and 0.5% (v/v) Tween-20 (Sigma, P1739) in PBS (Thermo Scientific, 14040091))across the plate. Fetuin coated plates were washed three times with Wash buffer (WB) (0.5% (v/v) Tween-20 in PBS) and serum dilutions were transferred to fetuin plates. Control wells with “pseudotype virus” only (equivalent to no NA inhibition) and SD only (equivalent to 100% NA inhibition) were also included. NA pseudotype virues was added to all wells except the SD control wells and plates were incubated overnight at 37°C. Next day, plates were washed six times and conjugate solution (1% (w/v) BSA, 1 µg/mL of lectin from *Arachis hypogaea* (peanut) peroxidase conjugate (Sigma L7759) in PBS (Thermo Scientific, 14040091)) was added. Plates were incubated while shaking (350 rpm) for 2 hours. After incubation, Plates were washed and 1-Step™ Ultra TMB-ELISA Substrate Solution (Thermo Fisher, 34029) was added. The plates were incubated for 10 minutes and reaction was stopped by adding 0.5 M HCl (Acros Organics, 124630025). The plates were read at optical density (O.D.) 450 nm

using Microplate reader (Agilent, BioTek 800 TS). The IC_{50} was determined as the inverse of serum dilution that resulted in 50% inhibition of NA activity using GraphPad Prism 10.4.1.

Hemagglutination Inhibition Assay (HAI)

To remove non-specific hemagglutination inhibitors, sera underwent a pre-treatment process. In brief, one volume of serum was mixed with three volumes of receptor-destroying enzyme (RDE) Seiken (DebenDiagnosticsLtd, 370013) and incubated for 12-18 hours at 37°C, followed by an inactivation step at 56°C for 30 minutes. The solution was diluted by addition of six volumes of PBS to reach a starting dilution of the serum of 1:10 (3.32 Log_2). The HAI tests were conducted in accordance with standard procedures[61], using four hemagglutinating units of virus (**Supplementary Table 9**) with 0.5% chicken erythrocytes. For the purposes of statistical analysis and graphic representation, a value of 1:5 (2.32 Log_2) was assigned to negative samples.

ELISpot

To quantify IFN-γ-secreting T cells, we employed an ELISpot assay adhering to Mabtech's Ferret IFN-γ ELISpot Plus kit protocol (Mabtech 3112-4APW-2). Fresh peripheral blood mononuclear cells (PBMC) were isolated using vacutainer CPT tubes (BD Biosciences, 362753), washed with PBS and resuspended in complete RPMI 1640 medium (ThermoFisher, 21875034) supplemented with 10% FBS, 1% penicillin-streptomycin, and 1% L-glutamine. Pre-coated plates were conditioned with RPMI 1640 medium containing 10% serum for 30 minutes at room temperature. Cells were stimulated under three conditions: PMA/Ionomycin ($1x10^5$ cells/well), Whole Inactivated Virus ($2x10^5$ cells/well, 100 HAU/mL of A/chicken/Italy/23VIR3799-1/2023 (H5N1)), and unstimulated controls ($2x10^5$ cells/well). Cells were plated in triplicate in complete RPMI and incubated for 24 hours at 37°C, 5% CO_2. Following incubation, plates were washed with PBS and detection antibody (MTF19-biotin, 0.5 µg/mL) was added. After washing again, streptavidin-alkaline phosphatase (ALP, 1:1000) was added to each well. BCIP/NBT-plus substrate solution was added for spot development, and plates were incubated at room temperature in the dark until spots became visible. The reaction was stopped by rinsing the plates with water. Spot-forming units (SFU) were quantified using an automated ELISpot reader (CTL-Immunospot S6 Ultra Analyzer). The relative ELISpot response was calculated as the ratio of the mean SFU from whole inactivated virus-stimulated samples to the mean SFU from unstimulated samples.

Detection of M2-binding antibodies via Luminex multiplex assay

Detection of M2 binding antibodies was done via Luminex assay. Recombinant Influenza A H5N1 M2 protein (A/chicken/Hebei/326/2005 (H5N1) (Accession- ABC74394.1)) (Stratech, LS-G56682-LSP) was coupled to Bio-Plex Pro™ magnetic COOH beads (Bio-Rad, MC1-0014-01) using Adipic acid dihydrazide (ADH) (Sigma-Aldrich, A0638). Negative control beads (Bio-Rad, MC1-0100-01) that were not coupled to any protein were also included. In a U-bottom microplate, 50 µL of sera was diluted in 1% (w/v) milk in PBS. The Nunc black plates (Greiner bio-one, 655077) were placed on a Bio-Plex® Handheld Magnetic

Washer (Bio-rad, 171020100), 50 µL per well of $1.5x10^5$ coupled beads were vortexed, pooled and plated. The liquid was discarded and sera were transferred to the beads on the plate. Control wells consisting of 1:100 blocking buffer (0.5 mg/mL blocking solution (Candor-bioscience ,110125) and 0.05% (w/v) Sodium Azide (Sigma Aldrich, S2002) diluted in skimmed milk (Millipore, 70166-500G), were included. The plates were incubated with shaking (500 rpm) at 37°C for 2 hours. After incubation, plates were washed three times with Wash Buffer (WB) (0.05% (v/v) Tween-20 in PBS). Fifty microliters of anti-mouse (Abcam, ab97024) or anti-ferret (Novus Biologicals, NB7222PE) secondary antibody labelled with fluorescent phycoerythrin (PE) dye was added to the wells followed by incubation for 30 minutes. After incubation, plates were washed thrice with WB and read via the Bio-Plex 200 System (Bio-rad, United States). The data is reported as Median Fluorescence Intensity (MFI) minus background, with background being a no serum control plotted using a non-linear sigmoidal 4-point plot, where x is log fold-dilution of serum and y is the median fluorescence intensity.

Detection of Binding antibodies via Enzyme Linked Immunosorbent Assay (ELISA)

Strain-specific IgG ELISA

Nunc™ clear Maxisorp plates (Thermo Scientific™, 439454) were coated with 5 µg/mL Influenza Antigens (**Supplementary Table 10**) and incubated at 4°C. Next day, plates were washed thrice with WB (0.1% (v/v) Tween-20 in PBS), blocking buffer (0.2M (w/v) Tris-base (Fisher Scientific, 10103203), 1% (w/v) BSA in PBS) was added to the plates and incubated on shaking (300 rpm) at 37°C for 2 hours. Starting at 1:00 dilution, the ferret serum samples were serially diluted 5-fold in blocking buffer. These dilutions were transferred to the coated plates and incubated again as mentioned previously. Control wells with blocking buffer only were also included. The plates were washed thrice and secondary antibody, horseradish peroxidase conjugated anti-ferret IgG (1:2000) (Abcam, AB112770) was added to all wells and incubated for 1 hour. Plates were washed again and 1-Step™ Ultra TMB-ELISA substrate solution was added to the plates and timed for 2 minutes. 0.5 M HCL was added to stop the reaction. The plates were read at optical density 450 nm (OD_{450}) using Microplate reader (Agilent, BioTek 800 TS).

IgG competition ELISA and Indirect ELISA

Serum were also assayed using two enzyme-linked immunosorbent assay (ELISA) kits, namely the ID Screen Influenza H5 Antibody Competition 3.0 Multi-Species (IDVet, FLUACH5V3 ver 0724 EN) and an in-house modified version of the ID Screen Influenza H5 Indirect (IDVet, FLUH5S ver 1221 EN). Both assays rely on the use of plates coated with an HA protein derived from a 2.3.4.4 clade virus.

The FLUACH5V3 ELISA kit was used in accordance with the manufacturer instructions adopting the protocol for chicken and turkey sera hence requiring a 1:2 dilution of serum (v/v) in Dilution Buffer 14 and an incubation in the microplate for one hour at 37°C. The results were expressed as S/N ratio % (positive S/N ≤ 60; doubtful 40<SN<60; negative S/N ≥ 40).

The indirect FLUH5S ELISA kit was modified to react with the ferret species and to ensure that the performance of the kit was in a linear range. Briefly, sera were diluted 1:3200 (v/v) in Dilution Buffer 14 and incubated in the microplate for one hour at 37°C. After removal of the samples and multiple washes, wells were incubated with an anti-dog HRP-conjugated antibody (available on request from IDvet) diluted 1:10 (v/v) in Dilution Buffer 1 (available on request from IDvet). For control wells, the kit HRP-conjugated antibody was used at a 1:10 dilution in Dilution Buffer 3 according to the instruction manual. The detection step was carried out by incubation of wells with 100 µL of the kit Substrate Solution followed by addition of 50 µL of the kit Stop Solution. The cut-off value was calculated using the standard formula "cut-off = mean Optical Density (O.D.) of negative controls + 3 × standard deviation"[62] and was set at an O.D. of 0.089. Archive sera collected from naïve ferrets were used as negative controls.

All ELISA assays were read with a Sunrise (Tecan) absorbance microplate reader and O.D. were recorded at 450 nm.

Microneutralisation assay (MN)

Pre-treated sera were tested by the microneutralisation assay (MN) according to the standard procedures described by the Center for Disease Control[63]. Two-fold dilutions of the treated sera were prepared in DMEM supplemented with 1% of a 2:3 penicillin-streptomycin solution (10,000 Unit/ml) (Euroclone-ECB3001D) and a 1:3 nystatin solution (Sigma-Aldrich, N1638) (10,000 Unit/ml), 10% BSA, 2% HEPES (Sigma-Aldrich, H0887). The dilutions were then mixed in a 1:1 (v/v) ratio with a virus solution containing 100 $TCID_{50}$/50 µL of the selected virus, and incubated for 1 hour at 37°C. To each well $1.5x10^4$ MDCK cells were added and incubated with the virus-serum mixture for 18-22 hours, at 37 °C with 5% CO_2. After incubation, cells were fixed with a cold 80% acetone solution and incubated for 1 hour at room temperature (RT) with a mouse anti-Influenza A monoclonal antibody mix (1:4000) (Merck Millipore, MAB8257 and MAB8258 1:1), in a 0.05% Tween-20 PBS solution. Cells were incubated for 1 hour with a secondary antibody followed by a 1-hour incubation with a peroxidase-labeled goat anti-mouse antibody (1:1000) (Jackson ImmunoResearch, 115-035-003) followed by a 5-10 minute incubation with a substrate based on o-phenylenediamine dihydrochloride (OPD) and citrate buffer. The reaction was stopped with a 0.5 N sulfuric acid solution. The optical absorbance of wells was read at 490 nm and calculations were made to identify the reciprocal of the highest serum dilution resulting in 50 % virus infection of cells.

Statistical analysis

All statistical analyses were performed with RStudio. A rank-based nonparametric test, the Wilcoxon rank sum test was used to determine if there were statistically significant differences among all groups. The Benjamini-Hochberg Procedure was applied to reduce the probability of false positives in the comparison of multiple groups.

Declarations

COMPETING INTERESTS

J.M.D., S.B.S., S.K.A., G.W.C., M.F., M.D., D.M., R.K., R.M., R.W., and J.L.H. are employees or shareholders of DIOSynVax Ltd. S.F. is an employee of Microsoft. The sequences of the DVX antigens have been patented under UK Patent Application No. GB2414517.8, Influenza vaccines, PCT/GB2022/052534, and PCT/GB2024/052670 (Influenza Antigen Synergies patent).

FUNDING

This research was funded by Bill and Melinda Gates Foundation: Grand Challenges Universal Influenza Vaccines Award: Ref: G101404 to J.L.H and Innovate UK, UK Research and Innovation (UKRI), for the project: Digital Immune Optimized and Selected Pan-Influenza Vaccine Antigens (DIOS-PIVa) Award Ref: 105078 to J.L.H.

AUTHOR CONTRIBUTIONS

S.V. and S.F. designed the vaccine antigens. B.A. and M.S. performed purification and preparation of DNA for antigen selection. N.T. provided key reagents. J.M.D., S.B.S., and S.K.A. produced DNA for immunisation and pseudotype viruses, performed *in vitro* assays, pMN, pELLA, flow cytometry, Luminex binding, and ELISA. G.W.C., P.T., and J.M.D. performed the mouse immunogenicity studies. R.B., T.T., and D.K conducted the mouse challenge experiments and post-mortem organ $TCID_{50}$ assays. L.V., S.R., V.M.P., E.M., A.F, and F.B. performed the ferret challenge and monitoring, virus production and infectivity, HAI, MN, ELISA, and dPCR. M.F. and M.P. performed and analysed T-cell ELISpots. A.L.O. scored tissue sections for pathology. M.V. performed immunohistochemistry. S.V., J.M.D., M.D., L.V., R.V., D.F., and F.B. analysed the data. S.V. and S.K.A. produced all figures. S.K.A., M.D., L.V., and F.B. performed statistical analyses. D.M. managed and coordinated all studies. R.K., R.M., R.W., and J.L.H. secured the funding. J.L.H conceptualised the investigation. J.M.D., F.B., and J.L.H designed the experiments. D.K., F.B., and J.L.H. supervised the project. S.V., J.M.D, S.B.S., and F.B. wrote the original draft. G.W.C., D.K., R.W., and J.L.H reviewed all data and edited the manuscript. All authors provided feedback on the paper.

ACKNOWLEDGEMENTS

We gratefully acknowledge all data contributors, the Authors and their Originating laboratories responsible for obtaining the specimens, and their Submitting laboratories for generating the genetic sequence and metadata and sharing via the GISAID Initiative, on which this research is based. We are thankful to etherna (Niel, Belgium) for providing us with formulated mRNA for these studies. We are

grateful to Dr. Francesco Gubinelli for providing us with the A/Astrakhan/3212/2020 (H5N8) antigen from Therapeutic Goods Administration Australia for our initial studies. We would like to acknowledge Professor Yoshihiro Kawaoka, University of Wisconsin-Madison, for kindly providing the A/Vietnam/1203/2004 H5N1 virus used for mouse challenge. We would also like to thank the Department of Pathology, University of Cambridge, UK, for the tissue sectioning and Haematoxylin and Eosin (H&E) staining of ferret tissues. We are also indebted to Professor John McCauley, Dr. Othmar Engelhardt, and Dr. Jason Long for their pre-submission reviews, advice, and feedback on this manuscript.

DATA AVAILABILITY

The main data supporting the results in this study are available within the paper and its Supplementary Information. The sequences used for designing the vaccine antigens were retrieved from the publicly available GISAID database. The sequences of the antigens have been patented under UK Patent Application No. GB2414517.8, Influenza vaccines, PCT/GB2022/052534 (Influenza Vaccines), and PCT/GB2024/052670 (Influenza Antigen Synergies patent).

References

1. Ly, H. Highly pathogenic avian influenza H5N1 virus infection of companion animals. *Virulence* 15, 2289780 (2024).
2. CDC. H5 Bird Flu: Current Situation. *Avian Influenza (Bird Flu)* https://www.cdc.gov/bird-flu/situation-summary/index.html (2025).
3. Cumulative number of confirmed human cases for avian influenza A(H5N1) reported to WHO, 2003–2024, 26 February 2024. https://www.who.int/publications/m/item/cumulative-number-of-confirmed-human-cases-for-avian-influenza-a(h5n1)-reported-to-who--2003-2024-26-february-2024.
4. Stimmelmayr, R., Rotstein, D., Torchetti, M. K. & Gerlach, R. Highly Pathogenic Avian Influenza Virus A(H5N1) Clade 2.3.4.4b Infection in Free-Ranging Polar Bear, Alaska, USA. *Emerg. Infect. Dis.* 30, (2024).
5. Agüero, M. *et al.* Highly pathogenic avian influenza A(H5N1) virus infection in farmed minks, Spain, October 2022. *Eurosurveillance* 28, (2023).
6. Lindh, E. *et al.* Highly pathogenic avian influenza A(H5N1) virus infection on multiple fur farms in the South and Central Ostrobothnia regions of Finland, July 2023. *Eurosurveillance* 28, (2023).
7. Mostafa, A. *et al.* Avian influenza A (H5N1) virus in dairy cattle: origin, evolution, and cross-species transmission. *mBio* 15, e02542-24 (2024).
8. Leguia, M. *et al.* Highly pathogenic avian influenza A (H5N1) in marine mammals and seabirds in Peru. *Nat Commun* 14, 5489 (2023).
9. Domańska-Blicharz, K. *et al.* Outbreak of highly pathogenic avian influenza A(H5N1) clade 2.3.4.4b virus in cats, Poland, June to July 2023. *Eurosurveillance* 28, (2023).

10. Moreno, A. *et al.* Asymptomatic infection with clade 2.3.4.4b highly pathogenic avian influenza A(H5N1) in carnivore pets, Italy, April 2023. *Eurosurveillance* 28, (2023).
11. Graziosi, G., Lupini, C., Catelli, E. & Carnaccini, S. Highly Pathogenic Avian Influenza (HPAI) H5 Clade 2.3.4.4b Virus Infection in Birds and Mammals. *Animals* 14, 1372 (2024).
12. He, M. *et al.* The H5N6 Virus Containing Internal Genes From H9N2 Exhibits Enhanced Pathogenicity and Transmissibility. *Transboundary and Emerging Diseases* 2025, 6252849 (2025).
13. Gao, F., Wang, Q., Qiu, C., Luo, J. & Li, X. Pandemic preparedness of effective vaccines for the outbreak of newly H5N1 highly pathogenic avian influenza virus. *Virologica Sinica* (2024) doi:10.1016/j.virs.2024.11.005.
14. Peacock, T. *et al.* The global H5N1 influenza panzootic in mammals. *Nature* (2024) doi:10.1038/s41586-024-08054-z.
15. Paulos, A. P. *et al.* Detection of Hemagglutinin H5 influenza A virus RNA and model of potential inputs in an urban California sewershed. 2024.12.31.24319823 Preprint at https://doi.org/10.1101/2024.12.31.24319823 (2025).
16. Wolfe, M. K. *et al.* Detection of Hemagglutinin H5 Influenza A Virus Sequence in Municipal Wastewater Solids at Wastewater Treatment Plants with Increases in Influenza A in Spring, 2024. *Environ. Sci. Technol. Lett.* 11, 526–532 (2024).
17. Feldman, J. *et al.* Human naïve B cells recognize prepandemic influenza virus hemagglutinins. *Sci. Immunol.* 10, eado9572 (2025).
18. Sun, W. *et al.* Clade 2.3.4.4 H5 chimeric cold-adapted attenuated influenza vaccines induced cross-reactive protection in mice and ferrets. *Journal of Virology* 97, e01101-23 (2023).
19. Hu, Y.-F., Zhang, B.-Z., Chu, H. & Huang, J.-D. Distinct evolution patterns of influenza viruses and implications for vaccine development. *The Innovation* 6, 100739 (2025).
20. Vishwanath, S. *et al.* A computationally designed antigen eliciting broad humoral responses against SARS-CoV-2 and related sarbecoviruses. *Nat. Biomed. Eng* 1–14 (2023) doi:10.1038/s41551-023-01094-2.
21. Sagulenko, P., Puller, V. & Neher, R. A. TreeTime: Maximum-likelihood phylodynamic analysis. *Virus Evol* 4, vex042 (2018).
22. Hadfield, J. *et al.* Nextstrain: real-time tracking of pathogen evolution. *Bioinformatics* 34, 4121–4123 (2018).
23. Khare, S. *et al.* GISAID's Role in Pandemic Response. *China CDC Wkly* 3, 1049–1051 (2021).
24. Elbe, S. & Buckland-Merrett, G. Data, disease and diplomacy: GISAID's innovative contribution to global health. *Glob Chall* 1, 33–46 (2017).
25. Shu, Y. & McCauley, J. GISAID: Global initiative on sharing all influenza data – from vision to reality. *Euro Surveill* 22, 30494 (2017).
26. NCBI Virus. https://www.ncbi.nlm.nih.gov/labs/virus/vssi/#/.

27. Del Rosario, J. M. M. *et al.* Exploiting Pan Influenza A and Pan Influenza B Pseudotype Libraries for Efficient Vaccine Antigen Selection. *Vaccines* 9, 741 (2021).
28. Carnell, G. W., Trombetta, C. M., Ferrara, F., Montomoli, E. & Temperton, N. J. Correlation of Influenza B Haemagglutination Inhibiton, Single-Radial Haemolysis and Pseudotype-Based Microneutralisation Assays for Immunogenicity Testing of Seasonal Vaccines. *Vaccines (Basel)* 9, (2021).
29. Carnell, G. W. *et al.* SARS-CoV-2 Spike Protein Stabilized in the Closed State Induces Potent Neutralizing Responses. *Journal of Virology* 95, 10.1128/jvi.00203 – 21 (2021).
30. Nadesalingam, A. *et al.* Paucity and discordance of neutralising antibody responses to SARS-CoV-2 VOCs in vaccinated immunodeficient patients and health-care workers in the UK. *The Lancet Microbe* 2, e416–e418 (2021).
31. Da Costa, K. A. S. *et al.* Influenza A (N1-N9) and Influenza B (B/Victoria and B/Yamagata) Neuraminidase Pseudotypes as Tools for Pandemic Preparedness and Improved Influenza Vaccine Design. *Vaccines* 10, 1520 (2022).
32. Pardi, N., Hogan, M. J., Porter, F. W. & Weissman, D. mRNA vaccines — a new era in vaccinology. *Nat Rev Drug Discov* 17, 261–279 (2018).
33. Wang, C. & Yuan, F. A comprehensive comparison of DNA and RNA vaccines. *Advanced Drug Delivery Reviews* 210, 115340 (2024).
34. Cagigi, A. & Douradinha, B. Have mRNA vaccines sentenced DNA vaccines to death? *Expert Review of Vaccines* (2023).
35. Caserta, L. C. *et al.* Spillover of highly pathogenic avian influenza H5N1 virus to dairy cattle. *Nature* 634, 669–676 (2024).
36. Jassem, A. N. *et al.* Critical Illness in an Adolescent with Influenza A(H5N1) Virus Infection. *New England Journal of Medicine* 392, 927–929 (2025).
37. Signore, A. V. *et al.* Neuraminidase reassortment and oseltamivir resistance in clade 2.3.4.4b A(H5N1) viruses circulating among Canadian poultry, 2024. *Emerging Microbes* & *Infections* 2469643 doi:10.1080/22221751.2025.2469643.
38. Tsybalova, L. M. *et al.* Development of a candidate influenza vaccine based on virus-like particles displaying influenza M2e peptide into the immunodominant region of hepatitis B core antigen: Broad protective efficacy of particles carrying four copies of M2e. *Vaccine* 33, 3398–3406 (2015).
39. Kavishna, R. *et al.* A single-shot vaccine approach for the universal influenza A vaccine candidate M2e. *Proceedings of the National Academy of Sciences* 119, e2025607119 (2022).
40. Neirynck, S. *et al.* A universal influenza A vaccine based on the extracellular domain of the M2 protein. *Nat Med* 5, 1157–1163 (1999).
41. Sakala, I. G., Honda-Okubo, Y., Li, L., Baldwin, J. & Petrovsky, N. A M2 protein-based universal influenza vaccine containing Advax-SM adjuvant provides newborn protection via maternal or neonatal immunization. *Vaccine* 39, 5162–5172 (2021).

42. Belser, J. A., Katz, J. M. & Tumpey, T. M. The ferret as a model organism to study influenza A virus infection. *Dis Model Mech* 4, 575–579 (2011).
43. Rioux, M. *et al.* The Intersection of Age and Influenza Severity: Utility of Ferrets for Dissecting the Age-Dependent Immune Responses and Relevance to Age-Specific Vaccine Development. *Viruses* 13, 678 (2021).

Figures

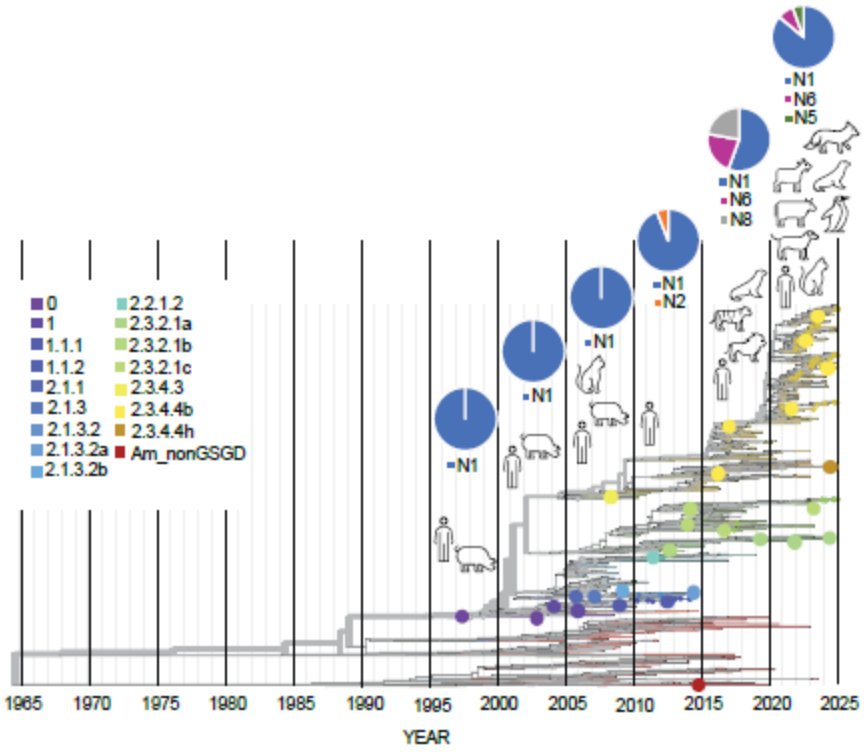


Figure 1

Temporal evolution of H5Nx in humans and mammals.

A timetree[21] representing temporal evolution of A/H5Nx was generated from Nextstrain[22] using 137 sequences from GISAID (**Supplementary Table 1**). The nodes of the tree are colour-coded according to the clade definition used by the Influenza H5 Working Panel in consultation with representatives of WHO, the Food and Agriculture Organization of the United Nations (FAO), the World Organisation for Animal Health (WOAH), and academic institutions, and are represented in the legend. Some of the nodes are represented as larger filled circles for visualisation and selected at random. The pie-charts represent the fraction of reassorted NA subtypes observed in the dataset in the timeframe (5 years) bound by thick vertical lines. The host of the H5Nx observed in the timeframe are represented as icons. A subset of hosts for time frame – 2021-2025 is shown for clarity.

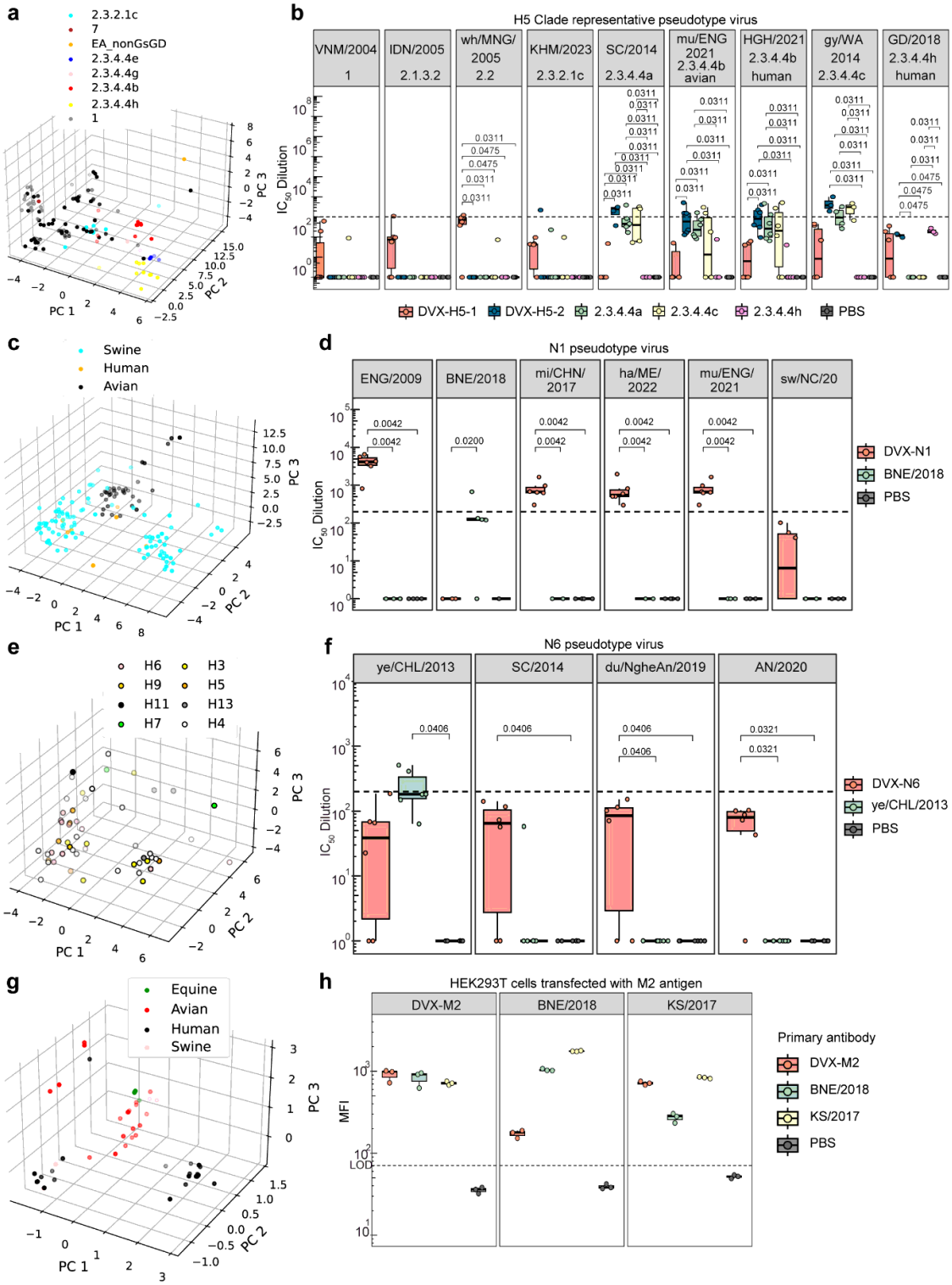


Figure 2

Immunogenicity of the computationally designed antigens in BALB/c mice.

a, Principal component (PC) plot showing non-redundant hemagglutinin H5 sequences from various A/H5 clades as individual color-coded dots. Analysis was used to generate two candidates, first, DVX-H5-1, that is phylogenetically closest to all the sequences in the dataset; and second, DVX-H5-2, that is

phylogenetically closest to all the sequences from the rapidly evolving clade 2.3.4.4 in the dataset. **b**, BALB/c mice were immunised with DVX-H5 antigen candidates and wild-type controls according to **Supplementary Table 2**. Neutralising titres as shown by terminal bleed serum IC_{50} (half-maximal dilution resulting in 50% neutralisation) values were determined via pseudotype neutralisation assay (pMN) against A/H5 pseudotyped viruses (**Supplementary Table 3**) representing the most relevant A/H5 clades. Dashed line indicates an IC_{50} value of 1000, a conservative baseline for a predicted protective immune response in a pMN[20,27–30]. **c**, PC plot showing a non-redundant dataset of neuraminidase N1 sequences from avian (black), human (orange), and swine (cyan) viruses. Sequences are predominantly from H1N1 and H5N1 virus strains. Analysis was used to generate a candidate – DVX-N1 that is phylogenetically closest to all the sequences in the dataset. **d**, BALB/c mice were immunised with DVX-N1 antigen candidate and wild-type control BNE/2018 according to **Supplementary Table 2**. Inhibition of N1 pseudotype viruses (**Supplementary Table 4**) are shown as IC_{50} dilution values determined using the pseudotype enzyme-linked lectin assay (pELLA). Dashed line indicates an IC_{50} value of 200, the predicted baseline for an effective neuraminidase inhibition response in this assay as described previously[31]. **e**, PC plot showing a non-redundant dataset of neuraminidase N6 sequences from the indicated HxN6 virus combinations. Analysis was used to generate a candidate – DVX-N6 that is phylogenetically closest to all the sequences in the dataset. **f**, BALB/c mice were immunised with the DVX-N6 antigen candidate and wild-type control ye/CHL/2013 (N6) according to **Supplementary Table 2**. Inhibition of N6 pseudotype viruses (**Supplementary Table 4**) are shown as IC_{50} dilution values determined via pELLA. **g**, PC plot showing a non-redundant dataset of Matrix protein 2 (M2) IAV sequences from human, equine, swine, and avian sources. Analysis was used to generate a candidate – DVX-M2 that is phylogenetically closest to all the sequences in the dataset. **h**, BALB/c mice were immunised with DVX-M2 antigen candidate and M2 wild-type controls from BNE/2018 (H1N1) and KS/2017 (H3N2) according to **Supplementary Table 2.** Flow cytometry binding data of HEK293T cells transfected with DVX-M2 and controls (vaccine antigens) against primary antibodies, post-vaccination sera from mice vaccinated with the respective antigens, are presented. The *y* axis represents binding as median fluorescence intensity (MFI). For each serum sample, three replicates of MFI are reported. Dotted line indicates the limit of detection (LOD) of the assay. For **b**, **d**, **f,** and **h**, the median and interquartile range of individual mouse serum samples are shown (n=6 per vaccination group). Statistical significance is shown by the indicated *p* values determined via two-way Wilcoxon rank test with Benjamini-Hochberg correction.

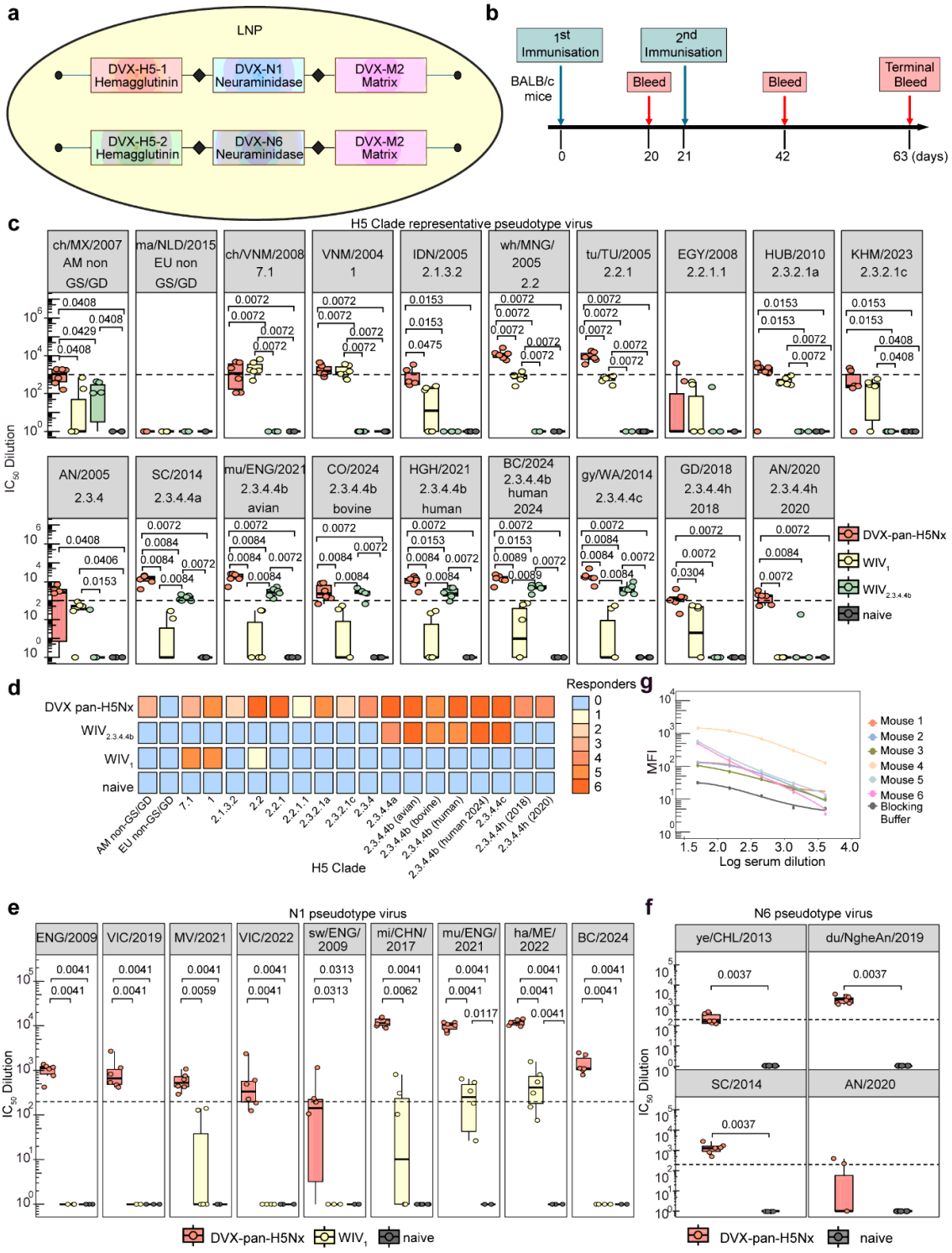


Figure 3

DVX-pan-H5Nx demonstrates broad immune responses compared to previously authorised CVV antigens for vaccine production in BALB/c mice.

a, Composition of the DIOSynVax first generation mRNA pan-H5Nx pre-pandemic vaccine antigen payload (VAP) - DVX-pan-H5Nx. DVX-pan-H5Nx is composed of two mRNA expression strings – (i) DVX-

H5-1_DVX-N1_DVX-M2, and (ii) DVX-H5-2_DVX-N6_DVX-M2. Each mRNA string was formulated into equal molar concentrations into one lipid nanoparticle (LNP). **b**, Immunisation and bleed schedule of mice vaccinated with DVX-pan-H5Nx and controls as stated in **Supplementary Table 5**. Terminal bleeds taken on D63 were used in subsequent serological investigations. **c**, Serum neutralising titres as shown by IC_{50} values determined by pMN against a H5 pseudotype virus (PV) panel (**Supplementary Table 3**) from mice vaccinated with DVX-pan-H5Nx, WIV_1 and $WIV_{2.3.4.4b}$. Dashed line indicates an IC_{50} value of 1000. **d**, Heatmap representation of immune responses of all immunisation groups against H5 PV from indicated clades. Legend indicates total mouse responders with an IC_{50} greater than 10^2 for each group. **e**, NAI titres against N1 PV (**Supplementary Table 4**) and **f**, N6 PV panels (**Supplementary Table 4**) as shown by IC_{50} values determined by pELLA of sera from mice immunised with DVX-pan-H5Nx and controls. Dashed line indicates an IC_{50} value of 200. **g**, Binding activity of M2-specific IgG antibodies, shown as MFI values, of serum from mice immunised with DVX-M2 against commercial recombinant M2 protein from A/chicken/Hebei/326/2005 (H5N1) as tested by Luminex Assay. Each sample (n=6) was tested in duplicate. For **c**, **e**, and **f**, the median and interquartile range of individual mouse serum samples are shown (n=6 per vaccination group). Statistical significance shown by the indicated *p* values was determined by two-way Wilcoxon rank test with Benjamini-Hochberg correction.

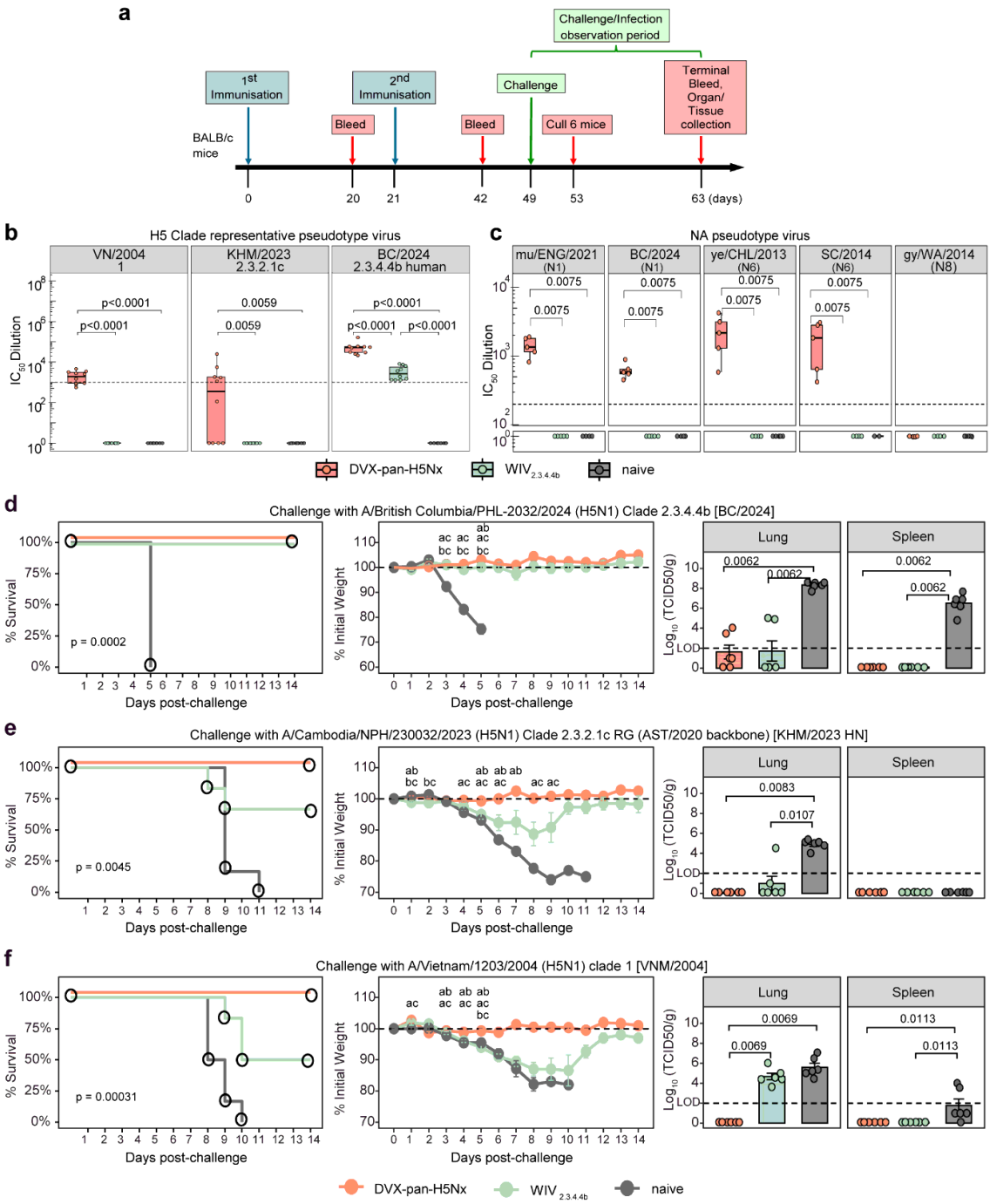


Figure 4

DVX-pan-H5Nx protects again multiple lethal H5N1 challenges and shows superior efficacy compared to a previously authorised CVV antigen for vaccine production in BALB/c mice.

a, Study schedule of mice vaccinated with DVX-pan-H5Nx and controls as detailed in **Supplementary Table 6**. **b**, Serum neutralising titres as shown by IC_{50} values determined by pMN against the selected

H5N1 challenge viruses from immunised mice taken on D42. Dashed line indicates an IC_{50} value of 1000. **c**, NAI titres against N1, N6, and N8 (**Supplementary Table 4**) PV panels as shown by IC_{50} values determined by pELLA of sera from mice immunised with DVX-pan-H5Nx and controls. Dashed line indicates an IC_{50} value of 200. **d-f, (1st panel)** Kaplan-Meier survival curves with *p* values indicating the result of Log-Rank (Mantel-Cox) test, **(2nd panel)** weights as monitored for all immunisation groups for 14 days and changes to initial weight indicated as % on the *y*-axis, and **(3rd panel)** tissue culture 50% infectious dose ($TCID_{50}$) values per gram of lung and spleen tissue collected 4dpc, are shown for all immunisation groups challenged with (**d**) A/British Columbia/PHL-2032/2024 (H5N1) (clade 2.3.4.4b) [BC/2024], (**e**) A/Cambodia/NPH230032/2023 (H5N1) (clade 2.3.2.1c) [KHM/2023HN], and (**f**) A/Vietnam/1203/2004 (H5N1) (clade 1) [VN/2004]. For **b, c,** and **3rd panel d-f**, plots shows the median and interquartile range of individual mouse serum samples. Statistical significance shown by the indicated *p* values was determined by two-way Wilcoxon rank test with Benjamini-Hochberg correction. For **2nd panel d-f,** weights with statistically significant differences are indicated by ab, ac, and bc, with *p* values summarised in **Supplementary Table 7**.

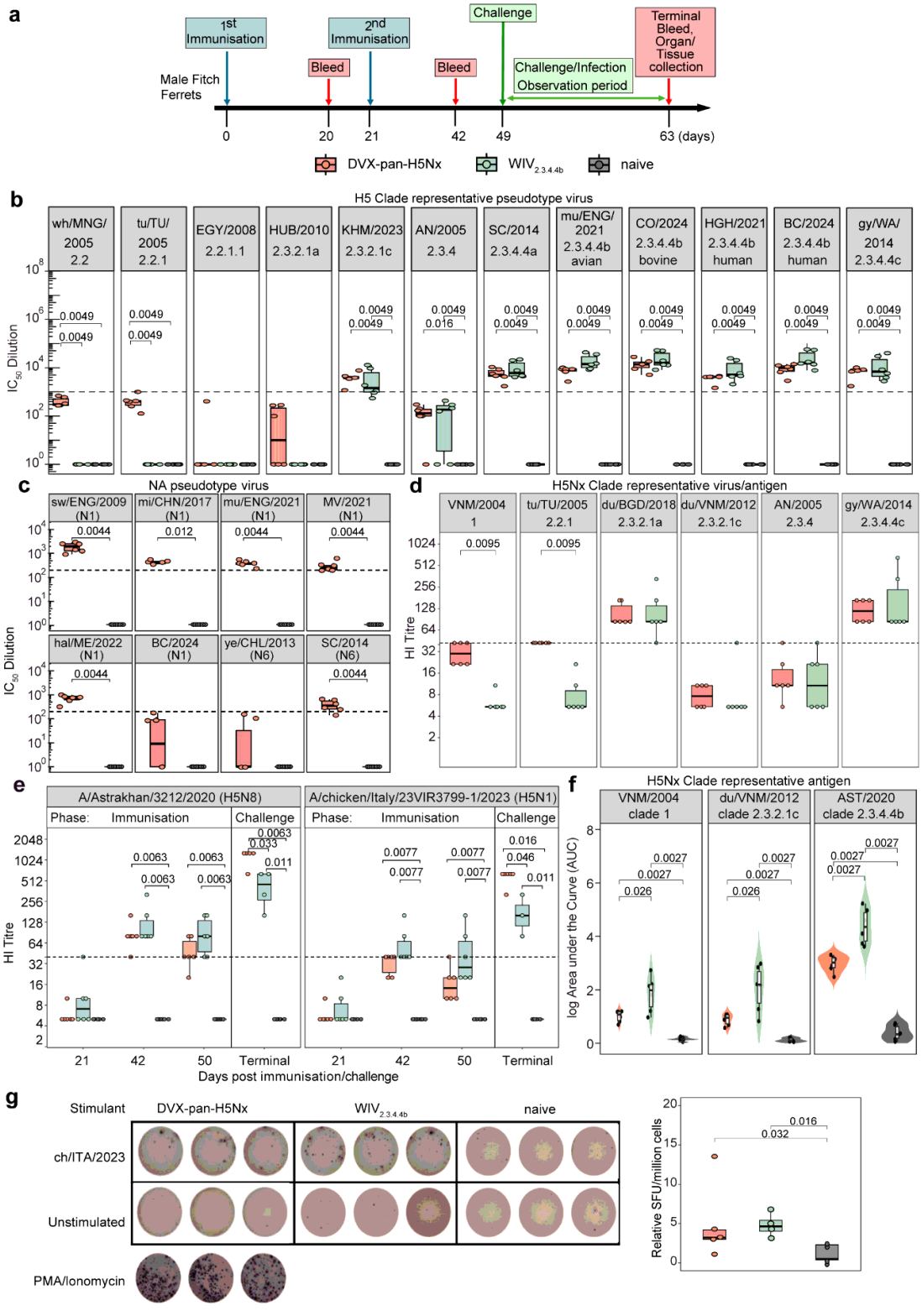


Figure 5

DVX-pan-H5Nx immunogenicity in ferrets.

a, Study schedule of ferrets vaccinated with DVX-pan-H5Nx and indicated controls as detailed in **Supplementary Table 7**. Bleeds taken on D42 were used for all subsequent serological assays. Ferrets were challenged on D49 with the highly pathogenic A/chicken/Italy/23VIR3799-1/2023 (H5N1), a clade

2.3.4.4b H5N1 virus. **b**, Serum neutralising titres as shown by IC_{50} values determined by pMN against a H5 pseudotype virus panel (**Supplementary Table 3**) from immunised ferrets. Dashed line indicates an IC_{50} value of 1000. **c**, NAI titres against N1 and N6 (**Supplementary Table 4**) pseudotype virus panels as shown by IC_{50} values determined by pELLA of sera from ferrets immunised with DVX-pan-H5Nx and controls. Dashed line indicates an IC_{50} value of 200. **d**, Hemagglutination inhibition (HI) titres of sera from immunised ferrets against a H5 virus panel (**Supplementary Table 8**) representing various A/H5 clades. HI titres are expressed as the highest dilution of serum that inhibited hemagglutination completely. Dashed line indicates a HI titre of 40, the accepted threshold for a seroprotective response in this assay. **e**, HI titre monitoring on days 21, 42, and 50, and post-challenge (terminal) of all vaccination groups against A/Astrakhan/3212/2020 (H5N8), and the challenge virus, A/ chicken/Italy/23VIR3799-1/2023 (H5N1). Dashed line indicates a HI titre of 40. **f**, Strain-specific binding antibodies against antigens from relevant H5 clades (**Supplementary Table 10**) were also confirmed by ELISA. The *y* axis represents the mean square root of area under the curve (AUC) from ELISA binding curves. **g**, Representative wells showing spot-forming units (SFU) from various stimulations obtained by ELISpot are shown for all immunisation groups (left panel). Relative SFU per million cells obtained by ELISpot were plotted to measure antigen-specific T cells in ferret pBMCs (right panel). IFN-γ secretion is evaluated after stimulation with 100 HA units/mL of inactivated A/chicken/Italy/23VIR3799-1/2023 (H5N1) the challenge virus, indicated as ch/ITA/2023. All plots (except for **a**) show the median and interquartile range of individual ferret serum samples (n=6 per vaccination group). Statistical significance shown by the indicated *p* values is determined via two-way Wilcoxon with Benjamini-Hochberg correction.

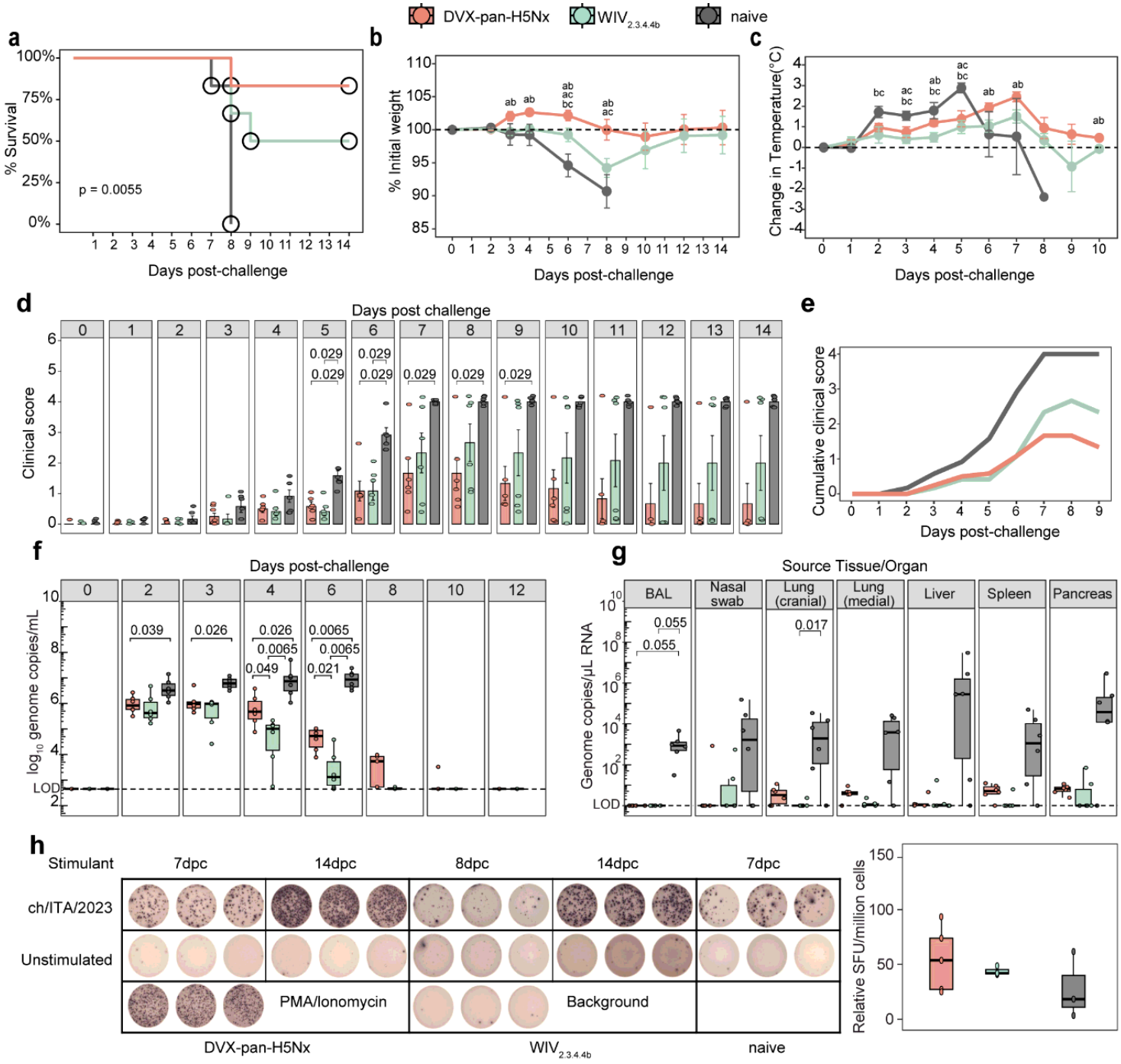


Figure 6

Superior efficacy of DVX-pan-H5Nx compared to $WIV_{2.3.4.4b}$ in a heterologous 2.3.4.4b challenge in ferrets.

a, Kaplan-Meier survival curves are shown for all immunisation groups during the 14-day challenge window. *p* value indicates the result of Log-Rank (Mantel-Cox) test among all groups. **b**, Weights were monitored for all immunisation groups for 14 days and changes to initial weight are indicated in % on the *y*-axis. Plot shows the mean values (n=6 ferrets/group) with standard deviation. Weights with statistically significant differences as determined by unpaired t-tests are indicated by ab, ac, and bc, with

p values summarised in **Supplementary Table 12**. **c**, Rectal temperature for all immunisation groups were monitored for 14 days and changes to baseline temperature (0dpc) are indicated on the *y*-axis. Plot shows the mean values (n=6 ferrets/group) with standard deviation. Rectal temperatures with statistically significant differences as determined by unpaired t-tests are indicated by ab, ac, and bc, with *p* values summarised in **Supplementary Table 13**. **d**, Clinical signs of infection in ferrets were recorded twice daily during the challenge window with a Clinical Score of 0 given to ferrets with no symptoms, and 4 to ferrets with severe symptoms resulting in culling. **e,** Cumulative clinical score for the ferret groups. **f**, Shedding of viral RNA from nasal washes was detected using droplet digital polymerase chain reaction (ddPCR). Nasal shedding is indicated as $\log_{10}$ genome copies/mL on the *y*-axis, with days post challenge (dpc) on the *x*-axis. From 8-12 dpc, only surviving ferret numbers per group are presented. The limit of detection (LOD) at 2.65 ($\log_{10}$ genome copies/mL) is indicated by a dashed line. **g**, Viral RNA in post-mortem tissues and organs was detected using ddPCR and is indicated as genome copies/µL RNA on the *y*-axis with days post challenge (dpc) on the *x*-axis. Viral RNA was extracted from samples on the day of culling for each individual ferret. LOD is indicated by dotted line. **h**, Representative wells showing spot-forming units (SFU) from various stimulations similar to **Fig. 5g** obtained by ELISpot are shown for all immunisation groups (left panel) . Days post-challenge when PBMCs were collected are indicated, with those obtained at 7dpc and 8dpc coming from ferrets from each vaccination group that were culled for reaching humane endpoints. Wells showing 14dpc indicate ferrets that survived the challenge. Relative SFU per million cells obtained by ELISpot were plotted to measure antigen-specific T cells in ferret PBMCs (right panel). For **d**, **f, g**, and **h**, plots show the median and interquartile range of individual ferret serum samples (n=6 per vaccination group). Statistical significance as shown by the indicated *p* values is determined via two-way Wilcoxon test with Benjamini-Hochberg correction.

Supplementary Files

This is a list of supplementary files associated with this preprint. Click to download.

- DVXH5NxSupplementaryfile090525.docx